THE SODIUM-HYDROGEN EXCHANGER NHX1 DRIVES LATE ENDOSOME-VACUOLE MEMBRANE FUSION

Mahmoud Karim

A Thesis
in
The Department
of
Biology

Presented in Partial Fulfillment of the Requirements
for the degree of Master of Science (Biology) at
Concordia University
Montreal, Quebec, Canada

September 2013

© Mahmoud Karim, 2013

CONCORDIA UNIVERSITY

School of Graduate Studies

This is to certify that the thesis prepared

By: Mahmoud Karim

Entitled: The Sodium-Hydrogen Exchanger NHX1 Drives Late Endosome-Vacuole Membrane Fusion

and submitted in partial fulfillment of the requirements for the degree of

Master of Science (Biology)

complies with the regulations of the University and meets the accepted standards with respect to originality and quality.

Signed by the final Examining Committee:

_____ Chair
Dr. Catherine Bachewich

_____ Examiner
Dr. Reginald Storms

_____ Examiner
Dr. William Zerges

_____ External Examiner
Dr. Vladimir Titorenko

_____ Supervisor
Dr. Christopher Brett

Approved by _____

Chair of Department or Graduate Program Director

_____ 2013 _____

Dean of Faculty

ABSTRACT

The Sodium-Hydrogen Exchanger Nhx1 Drives Late Endosome-Vacuole Membrane Fusion

Mahmoud Karim, M.Sc.

This dissertation reports the function of Nhx1, an endosomal Na^+ (K^+)/H^+ exchanger, in late endosome – vacuole membrane fusion in the model eukaryote *S. cerevisiae*. Nhx1 is found on the late endosome (LE) where it is known to play a pivotal role in endocytosis. Specifically, loss-of-function mutations in NHX1 block delivery of internalized surface proteins and newly synthesized proteins to the vacuole, the equivalent of the metazoan lysosome in yeast. Because membrane fusion between late endosomes and vacuoles is the final event necessary for protein delivery, and because Nhx1 binds Gyp6, a Rab-GTPase activating protein that is predicted to regulate membrane fusion, I hypothesized that Nhx1 may play a role in LE – vacuole membrane fusion. Unfortunately, there are no existing assays that directly measure this fusion event. Thus, to test this hypothesis, I first devised and optimized an *in vitro* LE – vacuole membrane fusion assay, which relies on the assembly of complementary β-lactamase fragments to form an active enzyme upon lumenal content mixing. I then used this biochemical assay to characterize the ions and protein machinery responsible for this fusion event. I then demonstrate that Nhx1 is important for LE-vacuole fusion, but its role in this process is independent of its interaction with Gyp6. Together, these results support a model of LE – vacuole fusion that requires H^+-transport by Nhx1 upstream of SNARE mediated bilayer mixing.

ACKNOWLEDGEMENTS

First and foremost, I am grateful to my mighty LORD for directing me towards Science and Knowledge.

I would like to thank from the bottom of my heart, my supervisor Dr. Brett for his patience and guidance that have made this project and thesis possible. I would also like to thank my committee members Drs. Storms and Zerges for their guidance and advice.

I would also like to thank Sevan Mattie for providing the TEM images herein, as well as my lab mates: Fellow graduate students Joël Richard, Dipti Patel, Mark Guterman, and lab manager Gabriel Lapointe for making the past two years a time to really remember!

TABLE OF CONTENTS

LIST OF FIGURES vii
LIST OF TABLES viii
LIST OF ABBREVIATIONS ix

INTRODUCTION 1
1. Yeast NHX1 to study neurodevelopmental disorders 1
2. Nhx1 and endocytosis 2
3. Late endosome-vacuole membrane fusion and Nhx1 3
MATERIALS AND METHODS 10
1. Plasmids 10
2. Yeast strains 11
3. Reagents 13
4. Membrane fractionation by sucrose gradient 15
5. Isolation of LEs and vacuoles from yeast 16
6. In vitro LE-vacuole fusion assay 16
7. Ypt7 extraction assay 17
8. Western Blot analysis 18
9. Fluorescence microscopy 19
10. Transmission Electron Microscopy 20
11. Data processing analysis 21

RESULTS 24
1. A Novel Cell-free assay to measure late endosome vacuole fusion events 24
2. Ionic requirements for LE-vacuole membrane fusion 25
3. Protein machinery required for late endosome-vacuole membrane fusion 28
4. H^+-transport by Nhx1 contributes to LE - vacuole fusion 31
5. Vam7 suppresses fusion defects caused by *nhx1*Δ 32
6. The Nhx1-Gyp6 interaction does not mediate LE - vacuole fusion 33
7. Ypt7 Rab activation is not impaired by the loss of NHX1 34

DISCUSSION 53

1. A new assay for late endosome-vacuole fusion in vitro 53
2. Protein machinery required for LE-vacuole fusion 54
3. Ion exchange by Nhx1 drives LE-vacuole fusion 55
4. Nhx1 regulates LE-vacuole fusion independent of its interaction with gyp6 56
5. Model Summarizing how Nhx1 and the fusion machinery regulate LE-vacuole fusion 57

REFERENCES 61

LIST OF FIGURES

Figure 1. Model describing how Nhx1 and Gyp6 regulate trafficking at the LE

Figure 2. Model describing how Nhx1 may promote Rab activation to drive LE membrane fusion

Figure 3. Cell-free late endosome membrane fusion

Figure 4. Reconstituted β-lactamase activity and membrane fusion

Figure 5. Ionic effects on LE-vacuole fusion

Figure 6. Effect of divalent cations on LE-vacuole fusion

Figure 7. Characterization of proteins that regulate LE-vacuole fusion

Figure 8. Ion transport by Nhx1 drives LE - vacuole fusion

Figure 9. Vam7 bypass fusion suppresses the *nhx1*Δ phenotype

Figure 10. Knocking out GYP6 has no effect on LE–vacuole fusion

Figure 11. Deletion of NHX1 does not cause Ypt7 inactivation

Figure 12. Model describing how Nhx1 may regulate LE-vacuole fusion

LIST OF TABLES

Table 1. Yeast expression plasmids used in this study

Table 2. Yeast strains used in this study

LIST OF ABBREVIATIONS

NHE, Na^+/H^+ Exchanger; LE, Late Endosome; TGN, Trans Golgi Network; HOPS, Homotypic fusion and vacuole Protein Sorting; GEF, Guanosine nucleotide Exchange Factor; GAP, GTPase Activating Protein; GDI: GDP-Dissociation Inhibitor; VPS, Vacuolar Protein Sorting; SNARE, Soluable *N*-ethylmaleimide-sensitive factor Attachment Protein Receptor; VAM, VAcuolar Morphogenesis; VMA, Vacuolar Membrane ATPase; CPY, Vacuolar carboxypeptidase Y.

INTRODUCTION

1. Yeast NHX1 to study neurodevelopmental disorders

Life requires that an organism regulates its cellular pH, volume, and ion composition to perform specific physiological processes (Brett et al., 2005). An important contributor to this cellular homeostasis is the family of secondary active ion transporters called Sodium Hydrogen Exchangers or NHEs that move monovalent cations in exchange for hydrogen ions across cellular membranes. Ion translocation is performed by a double 6 helix fold encoded by the N-terminus domain of NHE family proteins. A largely unstructured cytoplasmic C-terminus binds second messengers to couple activity to cellular signaling.

Based on sequence length, cation selectivity, drug sensitivity, and subcellular localization, the eukaryotic NHE family is divided into two distinct clades: plasma membrane (recycling and resident) and intracellular (endosomal/TGN, and plant vacuolar; Brett et al., 2005). Humans have nine NHE paralogs: NHE1-5 have orthologs in all metazoans, and are found on the plasma membrane where they interact with regulators of the actin cytoskeleton to drive changes in cellular morphology or motility by altering local pH gradients (Szaszi et al., 2002). Whereas NHE6-9 have orthologs in all eukaryotes, and reside on endosomes or the TGN where they contribute to luminal pH regulation but their cellular function remain uncharacterized (Collins & Wickner, 2007; Nakamura et al., 2005; Xinhan et al., 2011).

However in recent years, mutations in NHE6 and NHE9 have been linked to Autism Spectrum Disorders (ASDs; Franke et al., 2009; Morrow et al., 2008; Sommer

et al., 2011) . NHE6 and NHE9 are found within neuronal dendrites on mobile endosomes (Deane et al., 2013; Guterman & Brett, unpublished data) known to contribute to synaptic plasticity, a process that underlies learning and memory, behavior and cognition. Because defects that impair synaptic plasticity are thought to underlie ASDs (Toro et al., 2010), it is possible that loss-of-function mutations in NHE6 or NHE9 may impair endocytosis required for synaptic plasticity. But currently, we do not understand how NHE6 or NHE9 may drive endocytosis or how mutations lead to disease. For insight, we turn to the ancestor of NHE6 and NHE9, called Nhx1 in Baker's yeast, whose cellular functions have been studied in more detail.

2. Nhx1 and endocytosis

Like NHE6 and NHE9 in neurons, yeast Nhx1 predominantly resides on Late Endosomes (LE) where it imports Na^+ or K^+ into the lumen in exchange for export of H^+ into the cytoplasm. This function counteracts VMA activity to fine tune lumenal pH (Brett et al., 2005; Kojima et al., 2012; Nass, 1998). Further studies revealed that NHX1 (also called Vps44) plays a critical role in endocytosis (Bowers et al., 2000; Ali et al., 2004). Knocking out NHX1 results in the appearance of an enlarged Late Endosome (LE) where internalized surface proteins and biosynthetic cargoes accumulate because they get trapped en route to the vacuole (the yeast equivalent of the metazoan lysosome; Figure 1). Nhx1 transport activity is required for its role in endocytic trafficking, because point mutations that abolish ion transport show similar trafficking defects, and correcting lumenal hyperacidity observed in NHX1-knockout (nhx1Δ) cells suppresses endocytic defects (Bowers et al., 2000; Brett et al., 2005). As

protein cargo destined for the vacuole is normally sorted and packaged into intraluminal vesicles (ILVs) at the LE, it was originally hypothesized that deletion of NHX1 interfered with this process. However, ILV formation persists in nhx1Δ cells although vacuole delivery is impaired (Brett et al., 2011; Kallay et al., 2011). Thus an alternative explanation for the enlarged endosome found in nhx1Δ cells is that trafficking out of the LE is impaired. There are two trafficking pathways that leave the LE; The retrograde pathway to the TGN, mediating surface protein recycling, and the anterograde pathway to the vacuole for internalize surface protein degradation. Underlying both pathways is a LE fusion event, either at the TGN or vacuole. Because nhx1Δ cells have similar growth phenotypes as cells missing components of the vacuole fusion machinery (e.g. MON1, VAM7, VPS41, YPT7; Brett et al., 2011), I decided to focus my studies on the potential role of Nhx1 in LE-vacuole membrane fusion.

3. Late endosome-vacuole membrane fusion and Nhx1

Predominantly based on *in vitro* studies of homotypic yeast vacuole fusion as a model, we understand that organelle membrane fusion relies on an ordered cascade of protein mediated subreactions including priming, tethering, docking, and fusion to recognize, bridge, and eventually merge the opposing lipid bilayers (Figure 2). Starting with ''priming'', Sec18, an AAA ATPase, binds Sec17, a SNARE chaperone, and hydrolyzes ATP to disassemble cis-SNARE complexes (consisting of Vam3, Vti1, Vam7, and Nyv1), releasing it from the HOPS tethering complex (Mayer et al., 1996) - essentially resetting the fusion machinery for a new round of fusion. ''Tethering'' is

defined as when apposing vacuole membranes make first contact. This event is governed by Rabs, small Ras-like GTPases, that function analogous to molecular timer switches: GDP-bound Rabs require the activity of Guanine nucleotide Exchange Factors (or GEFs) to convert them into their active GTP-bound state, which persists until hydrolysis is initiated through interaction with a GTPAase Activating Protein (GAP) which converts the Rab-GTP back to the GDP-bound state (Figure 2B). Rab-GTP mediates tethering through homodimerization *in trans* (across membranes) and by interacting with downstream effectors like the HOPS protein holocomplex; Brett et al., 2008). The third stage of membrane fusion, called ''docking'', involves the recruitment of additional tethering factors to the initial contact site along with SNARE proteins required for membrane fusion (Kato and Wickner, 2001). These components organize themselves into an expanding ring called the vertex, at the contact site between the membranes. SNAREs present on opposing membranes interact *in trans* to form a tight four-helical complex by zippering from their soluble N-termini to their membrane anchored C-termini. Energy from SNARE assembly provides enough force to drive the phospholipid bilayers together resulting in complete membrane ''fusion'' and luminal content mixing.

But how does Nhx1 contribute to this process? In 2004, Rao and colleagues discovered that Nhx1 binds Gyp6, a Rab-GAP that inactivates the Rabs Ypt6 and Ypt7, which are implicated in LE fusion with the TGN and vacuole, respectively (Ali et al., 2004; Brett et al., 2008; Vollmer et al., 1999; Will & Gallwitz, 2001; Bensen et al., 2001; Balderhaar et al., 2010). Because knocking out GYP6 partially suppresses the trafficking defects observed in nhx1Δ cells, we derived a model whereby Nhx1 may

function to bind and inhibit Gyp6 to permit Rab activation required for LE fusion (Figure 1, bottom panel). Using this model, I predict that a loss-of-function mutation in NHX1 promotes Ypt7 inactivation by Gyp6 and blocks LE-vacuole fusion.

To test this hypothesis, I first devised and optimized a new cell free assay to quantify LE-vacuole fusion that relies on β-lactamase reconstitution upon luminal content mixing. I then characterized the fusion machinery required for this process. Because Nhx1 plays a critical role in pH and cation homeostasis, I also characterized the ionic requirements for LE-vacuole fusion, and discovered that they were distinct from homotypic vacuole fusion (HVF) and reflect Nhx1 activity. Finally, using this assay I demonstrate that knocking out NHX1 impairs LE-vacuole fusion, and that luminal hyperacidity is likely responsible, consistent with previous in vivo studies (Brett et al., 2005b). However, contrary to our predictions, knocking out GYP6 had no effect on LE-vacuole fusion, and knocking out NHX1 has no effect on the state of Ypt7 activation. Thus we discuss an alternative mechanism of Nhx1 mediated LE-vacuole fusion, and apply my results to predict how mutations in human NHE6 and NHE9 may cause disease.

Figure 1. Model describing how Nhx1 and Gyp6 regulate trafficking at the LE

Cartoons summarizing the effects of knocking out NHX1 on surface (blue) cargo trafficking, lumenal pH and late endosome morphology (wild type, top; nhx1Δ cells, bottom). Insets show Rab-GTPases important for membrane trafficking out of the LE, and the effects of knocking out NHX1 on their activity (Rab:GTP is active, Rab:GDP is inactive). ER, endoplasmic reticulum; TGN, trans-Golgi network; SV, secretory vesicle; PM, plasma membrane; CW, cell wall; EE, early endosome; LE, late endosome; Ste3, a surface G-protein-coupled receptor.

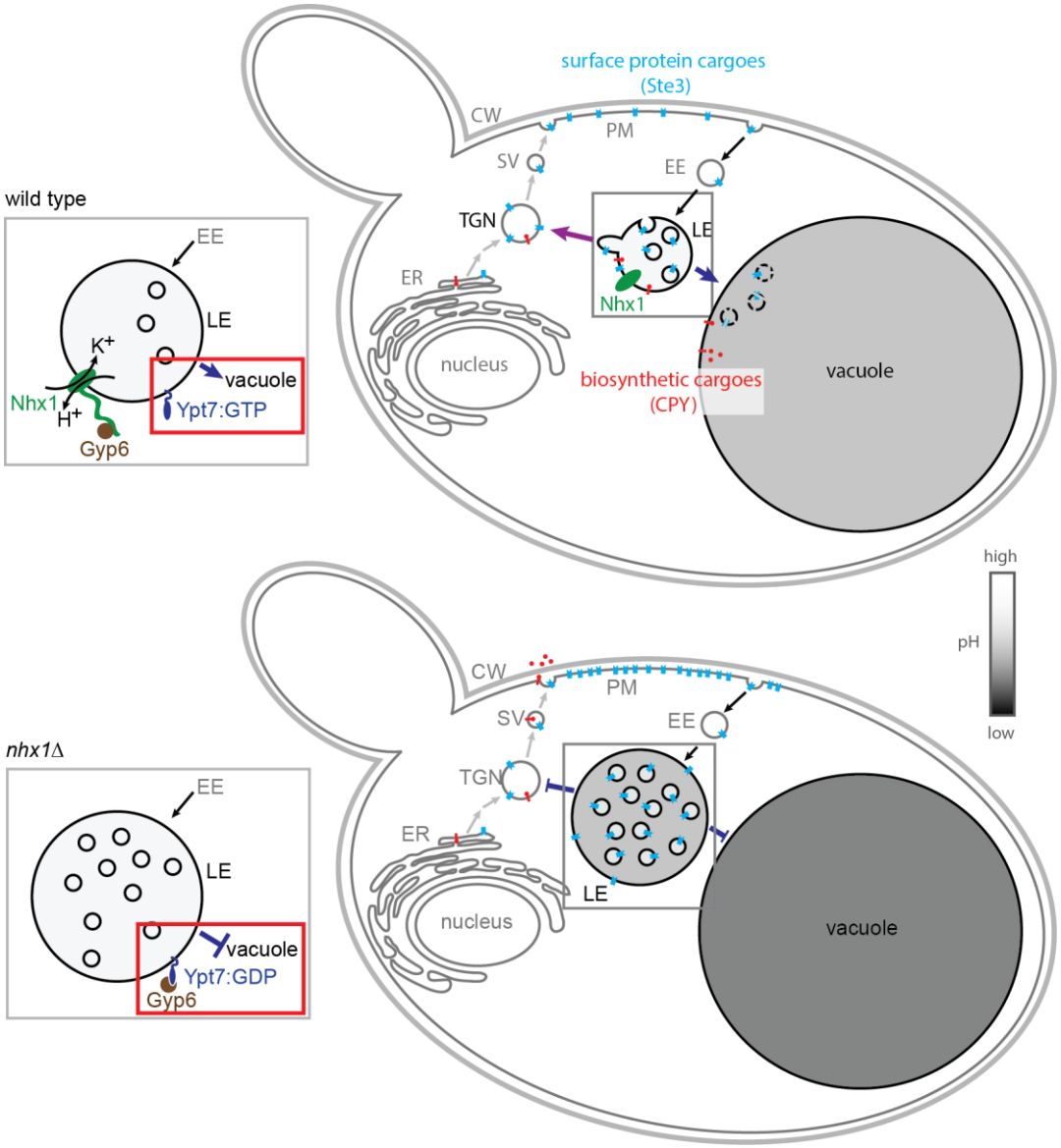
wild type
EE
LE
K+
Nhx1
H+
vacuole
Ypt7:GTP
Gyp6
surface protein cargoes
(Ste3)
CW
PM
SV
EE
TGN
LE
ER
Nhx1
nucleus
biosynthetic cargoes
(CPY)
vacuole
high
pH
low
nhx1Δ
EE
LE
vacuole
Ypt7:GDP
Gyp6
CW
PM
SV
EE
TGN
ER
LE
nucleus
vacuole

Figure 2. Model describing how Nhx1 may promote Rab activation to drive LE membrane fusion

(A) Cartoon illustrating the subreactions (or stages) and proteins necessary for LE-vacuole membrane fusion. Inhibitors of each subreaction are shown (α, anti; Ab, antibody). Addition of recombinant Vam7 initiates the reaction at the fusion stage, bypassing the requirement for Ypt7 activation. Nhx1 and Gyp6 likely control Ypt7-mediated tethering. (B) Cartoon illustrating the Rab cycle. GEF, Guanine nucleotide Exchange Factor; GAP, GTPase Activating Protein; NHE, $Na^+(K^+)/H^+$ Exchanger. Gdi1 acts as a chaperone to shuttle inactive Rab:GDP on and off membranes. (C) Table indicating proteins thought to drive LE-Vacuole fusion.

A

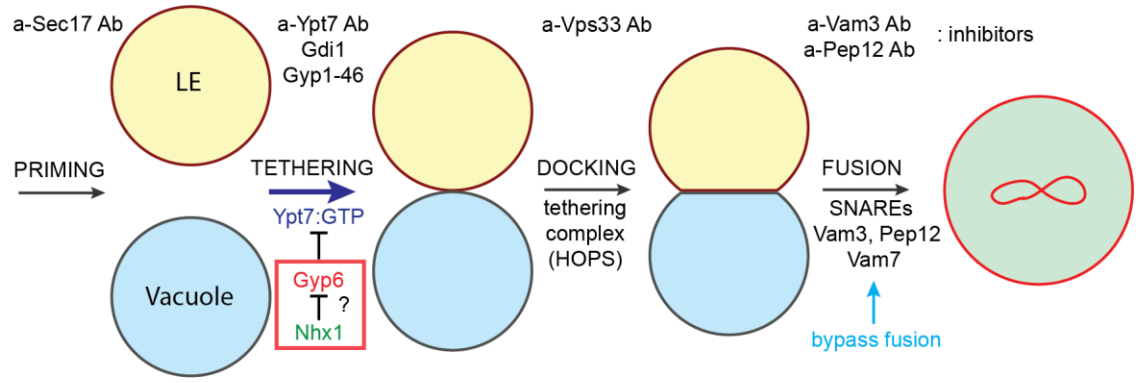

B

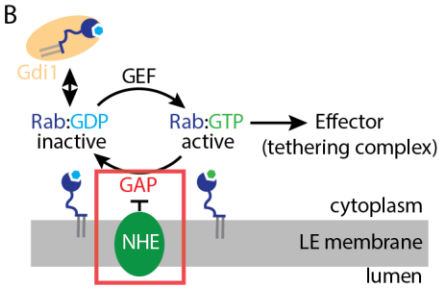

C

fusion protein	LE-V
Rab-GTPase	Ypt7
GAP	Gyp7 > Gyp6
GEF	Vps39
tethering complex (subunits)	HOPS? (Vps11,16,18,33,39,41)
syntaxin (SNARE)	Pep12
NHE	Nhx1

MATERIALS AND METHODS

1. Plasmids

All plasmids used in these studies are listed in Table 1. To generate lumenal probes for the LE-vacuole fusion assay, I amplified LE syntaxin ortholog Pep12 by PCR from genomic DNA isolated from wild type BY4742 cells using a forward primer flanked with a EcoRI restriction site 5'-GGAATTCATGTCGGAAGACGAATTTTTTG GTGG-3' and reverse primer flanked with a BamHI restriction site 5'CGGGATCCCAATTTCATAATGAGAAAAATAAAAAG-3'. I subcloned the PCR product into pYJ406-Fos-GS-ω, a plasmid encoding c-Fos fused to ω-fragment of *E. coli* β-lactamase and the N-terminal 50 amino acids of CPY (Jun and Wickner, 2007), replacing CPY50 with PEP12 to deliver the product to the LE. The final construct (pMK1) has Pep12-Fos-Gs-ω inserted between XhoI and SacI restriction sites in pRS406, an integrating yeast expression plasmid containing the URA3 as the selectable marker. To increase expression of the probe, I generated a second plasmid (pMK2) by cutting pMK1 with XhoI and SacI and ligating Pep12-Fos-Gs-ω into pRS404 (Sikorski and Hieter, 1989), an integrating plasmid containing the TRP1 auxotrophic marker.

To make complementary fusion probes, I amplified Jun-Gs-α by PCR from pYJ406-Jun-Gs-α, a plasmid encoding c-Jun fused to α-fragment of *E. coli* β-lactamase and the N-terminal 50 amino acids of CPY (Jun and Wickner, 2007), using the forward primer 5'CAGGGAAGATCTCACCCAGAAACGCTGGTGAAAGTAAAAGATGC-3' and the reverse primer 5'CAGTACGAGCTCCCGAGATTCATCAACTCATTGCTGGAGTT

AGC-3' flanked by BglII and SacI restriction sites, respectively. I then replaced Fos-Gs-ω in MK1 or MK2 with this PCR product to generate pMK3 and pMK4, respectively (BamHI and BglII have compatible cohesive ends). pYJ406-Fos-Gs-ω and pYJ406-Jun-Gs-α were gifts from William Wickner (Dartmouth College Hanover, NH, USA).

2. Yeast strains

All *Saccharomyces cerevisiae* strains used for these studies were derivatives of BY4742 (Invitrogen, Carlsbad, CA, USA), with the exception of BJ3505 and DKY6281 which are derivatives of SEY6210 (see Table 2). For LE-vacuole fusion assays, I transformed BJ3505 with pMK1 and pMK2, or pMK3 and pMK4 to generate BJ3505-Pep12-Fos (MKY2) and BJ3505-Pep12-Jun (MKY3), respectively each with two copies of the LE-localized fusion probe. Similar strains containing vacuole probes (BJ3505-CPY50-Fos and BJ3505-CPY50-Jun) were gifts from William Wickner (Dartmouth College Hanover, NH, USA). To examine the contribution of Nhx1 to LE-vacuole fusion, I knocked out NHX1 by replacing it with a KanMX cassette using the PCR product of a two-step PCR that first amplified KanMX from pFA6a-KanMX with homology to upstream and downstream UTRs flanking NHX1 with the forward primer 5'GGATAATCTTTTATCGCTGTCAGTACATACCATATGAAAACGGATCCCCGGGT TAATTAA-3' and the reverse primer 5'- ATATTTATATTAGAAACAAGGAAACCATACA CTTTAAAGTGAATTCGAGCTCGTTTAAAC-3', and then extended the homologous regions to 80 nucleotides using the forward primer 5'-GTTGTAGATTAAACATAGATT GCAAGCAGTGAAATTCAGAGGATAATCTTTTATCGCTT-3' and reverse primer 5'CGGCGTTGAGTAAGAGAGAATGTATAAAGACTTAATTAATATATTTATATTAGAAACA

AG-3'. I transformed the resulting PCR products into MKY2, MKY3, BJ3505-CPY50-Fos, or BJ3505-CPY50-Jun to generate a complementary set of nhx1Δ fusion strains: BJ3505-Pep12-Fos *nhx1Δ*::KanMX (MKY4), BJ3505-Pep12-Jun *nhx1Δ*::KanMX (MKY5), BJ3505-CPY50-Fos *nhx1Δ*::KanMX (MKY6), and BJ3505-CPY50-Jun *nhx1Δ*::KanMX (MKY7), respectively.

To knock out GYP6 in these fusion strains, I replaced GYP6 with the KanMX cassette using the PCR product of a two-step PCR that first amplified KanMX from pFA6a-KanMX with homology to upstream and downstream UTRs flanking GYP6 with the forward primer 5'GTTGTAGATTAAACATAGATTGCAAGCAGTGAAATTCAGA GGATAATCTTTTATCGCTGT-3' and reverse primer 5'-CGGCGTTGAGTAAGAGAGAAT GTATAAAGACTTAATTAATATATT TATATTAGAAACAAG-3', and then extended the homologous regions to 80 nucleotides using the forward primer 5'-ATGGGGGAGAGTTGTCAAGAGAATTGGCATACATAGAGAGGGTTAGCTGTCGTGCGTTT G-3' and reverse primer 5'-TTTTTTTTTTTTTGATTTTGTCGTGCGGGTGTGCAGGCTGG GATTTCAAACAAATAAAA-3'. I transformed the PCR product into MKY2, and BJ3505-CPY50-Jun to generate complementary fusion strains BJ3505-Pep12-Fos *gyp6Δ*::KanMX (MKY8), and BJ3505-CPY50-Jun *gyp6Δ*::KanMX (MKY9), respectively.

To knock out GYP6 from *nhx1Δ* fusion strains, I first swapped the KanMX marker for NatMX in MKY4 and MKY7 strains by transforming them with linearized MS18; an integrating plasmid with NatMX flanked by the UTRs upstream and downstream KanMX, a gift from Michael Sacher (Concordia University, Montreal, QC). I then transformed the new strains BJ3503-Pep12-Fos *nhx1Δ*::NatMX (MKY10) and BJ3505-CPY50-Jun *nhx1Δ*::NatMX (MKY11) with the PCR product used to replace GYP6 with

KanMX to generate complementary fusion strains BJ3505-Pep12-Fos *nhx1Δ*::NatMX *gyp6Δ*::KanMX (MKY12) and BJ3505-CPY50-Jun *nhx1Δ*::NatMX *gyp6Δ*::KanMX (MKY13).

To examine the subcellular distribution of Nhx1, GFP was inserted into the genome in frame behind the NHX1 gene by homologous recombination (Longtine et al., 1998): BJ3505 cells were transformed with the product of a two-step PCR that first amplified GFP-URA3 from pFA6a-GFP-URA3 with homology to NHX1 C-terminal and downstream UTR flanking URA3 with the forward primer 5'GGCTACGCAATCACCTGCAGATTTCTCTTCCCAAAACCACCGGATCCCCGGGTTAATTA A-3′ and reverse primer 5′-GGATAATCTTTTATCGCTGTCAGTACATACCATATGAAAA CGGATCCCCGGGTTAATTAA-3′, and then extended the homologous regions to 80 nucleotides using the forward primer 5'-CAGTATTCTTGGACAACGTTTCTCCATCCTTACAAGATTCGGCTACGCAATCACCTGCAG-3' and reverse primer 5'- CGGCGTTGAGTAA GAGAGAATGTATAAAGACTTAATTAATA TATTTATATTAGAAACAAG-3'. I transformed the PCR products into BJ3505 to generate BJ3503 NHX1::GFP (MKY1). Unless otherwise noted, yeast were grown in either rich YPD medium (1% yeast extract, 2% peptone, 2% dextrose) or in minimal SC medium (2% glucose, 0.5 % ammonium sulfate, 0.17% yeast nitrogen base without amino acids, with or without the addition of Histidine (30 μg/ml), Leucine (0.1 mg/ml), Uracil (30 μg/ml), and Lysine (0.1 mg/ml).

3. Reagents

All yeast and bacteria growth media was purchased from BIOSHOP (Bioshop Canada Inc, Burlington, ON). All other buffers and reagents were purchased from Sigma Chemical Company (St. Louis, MO, USA), with the exception of Ficoll (GE Healthcare, Tokyo, Japan); Nitrocifin (Calbiochem, San Diego, CA, USA); FM4-64 and fluorescently labeled secondary antibodies (Invitrogen, Carlsbad, CA, USA); AEBCF and ATP (Roche, Indianapolis, IN, USA); or the Bradford Assay Kit (Pierce, Merseyside Drive, Mississauga, ON). All primers were purchased from Integrated DNA Technologies (Coralville, IA, USA), and DNA sequencing was performed at the Centre d'Innovation Génome Québec (McGill University, Montreal, QC). All restriction enzymes, Ni-sepharose 6FF, and glutathione sephraose 4B, polymerases, and ligases were purchased from New England Biolabs (County Rd, Ipswich, MA, USA). Most consumables (e.g. amicon centrifugal filters) were purchased from Fisher (Fair lawn, NJ, USA) or VWR (Radnor, PA, USA).

Purified rabbit polyclonal antibody against Sec17 was a gift from William Wickner (Dartmouth College Hanover, NH, USA) whereas those against Vam3, Ypt7, Vps21, Vps33, Vps41, Vps10 and CPY were gifts from Alexey Merz (University of Washington, Seattle, WA, USA). Recombinant mouse antibody against Pep12 was purchased from Invitrogen (Mainway, Burlington, ON). Recombinant rabbit IgG against GFP was purchased from Abcam (Toronto, ON). Recombinant Intein-Gdi1, Gyp1-46 6xHis, GST-Fos, and lyticase were expressed in *E.coli*, and purified by affinity chromatography as described (Starai et al., 2007; Lo et al., 2011; Kreis et al., 2005; Shens et al., 1991). *E.coli* (BL21, de3) expressing Intein-Gdi1 or Gyp1-46 6xHis were gifts from Alexey Merz (University of Washington, Seattle, WA, USA); strains expressing GST-Fos or

lyticase were gifts from William Wickner (Dartmouth College Hanover, NH, USA). Purified recombinant Vam7 protein stock were gifts from Alexey Merz (University of Washington, Seattle, WA, USA). All protein and antibody reagents added to fusion reactions were exchanged into PS buffer, aliquoted, flash frozen in liquid nitrogen, and stored at -80 ^{o}C until use. All fusion reagent stocks were prepared in PS buffer.

4. Membrane fractionation by sucrose gradient

Yeast cells were grown in YPD overnight to OD_{600nm} 1.6/ml, harvested, and spheroplasted with lyticase for 30 min at 30 ^{o}C. Spheroplasts were then sedimented and resuspended in 10 ml of TEA buffer (10 mM triethanolamine, pH 7.5, 100 mg/ml phenylmethylsulfonyl fluoride, 10 mM NaF, 10 mM NaN_3 ,1 mM EDTA, and 0.8 M sorbitol) and homogenized on ice by Dounce homogenization (20 strokes). Cell lysates were centrifuged at 15,000 g for 20 min, and the resulting supernatant was then centrifuged at 100,000 g for 2 h to sediment cellular membranes. Pellets were resuspended in 1 ml of TEA buffer and loaded onto a stepwise (20–70%) sucrose density gradient, and then centrifuged at 100,000 g for 16 h at 4 °C to separate different cellular membranes by density. Samples were collected from the top, and each fraction was precipitated using 10% trichloroacetic acid, washed and resuspended in 100 µl of SDS-PAGE buffer. Fractions were then loaded into 15 well SDS-polyacrylamide gels and subjected to electrophoresis to separate proteins by size. Western blot analysis was performed to determine the fractions that contain proteins of interest.

5. Isolation of LEs and vacuoles from yeast

Yeast strains, each expressing a different fusion probe targeting late endosomes or vacuoles, were grown overnight in 1 L of YPD to 1.4 -1.8 OD_{600nm} units/ml, harvested and the pellet was then washed with 50 ml of wash buffer (0.5 μM DTT, 50 mM Tris-HCl pH=9.4) for 10 min at 30°C. To break their cell walls, cells were then collected and resuspended in 15 ml spheroplasting buffer (20 mM potassium phosphate pH 6.8 and 200 mM Sorbitol in diluted YPD medium) with 1 μg/ml zymolayaze, and incubated for 30 min at 30°C. The results spheroplasts were collected, resuspended in 15% ficoll in PS buffer (20 mM PIPES pH 6.8, 200mM sorbitol), and treated with DEAE dextran to gently lysis the plasma membranes. Permeablized spheroplasts were then transferred to SW41-Ti centrifuge tubes, covered with a 3 step ficoll gradient of 8%, 4%, and 0% layers, and centrifuged at 125,000 g for 90 min at 4˚C. Purified LE and vacuoles were harvested from the 4-0% interphase (Haas et al., 1994), and organelle protein concentration was estimated by Bradford assay.

6. In vitro LE-vacuole fusion assay

LEs and vacuoles were isolated from yeast expressing the chimeric protein CPY50-Jun-GS-α targeted to vacuoles, or Pep12-Fos-Gs-ω targeted to LEs. 6 μg of organelles from each strain was added to standard 60 μl fusion reactions containing 125 mM KCl, 5 mM MgCl2, ATP regenerating system (1 mM ATP, 40 mM creatine phosphate, 0.5

mg/ml creatine kinase), 10μM CoA in PS buffer, and supplemented with 11 μM recombinant GST-Fos protein to reduce background caused by possible organelles lysis (Jun & Wickner, 2007). Where indicated, the pH of the reaction buffer was changed by titration with either 1M HCl or 1M KOH, and KCl was replaced with equimolar NaCl, NH_4Cl, RbCl, or KoAc. Osmotic shock was applied by adjusting reaction sorbitol to values between 100 and 1000 mM. Bypass fusion was stimulated by replacing ATP-RS with 100 nM purified recombinant Vam7 protein in the presence of 10 μg/ml bovine serum albumin. Fusion reactions without ATP, or without incubation (90 min on ice) were used as negative controls. To block fusion, either antibodies raised against Sec17, Ypt7, Vps21, Vps33, Vam3, Pep12, or purified recombinant Gdi or Gyp1-46 (0.05-7.0 μM), were added to fusion reactions as indicated. Reactions were incubated for 90 min at 27°C then stopped by placing them on ice. LE-vacuole fusion was quantified by adding the reaction to 140 μl of nitrocefin developing buffer (100 mM NaPi pH 7.0, 150 μM nitrocefin, 0.2% Triton X-100) in a 96-well clear bottom plate. To measure nitrocefin hydrolysis, absorbance at 492 nm was monitored at 15 seconds intervals for 5-10 min at 30°C with a Synergy H1 plate-reading, multimode spectrophotometer (Bioteck, Winooski, VT, USA). A blank reference well containing 140 μl developing buffer and 12 μg isolated organelles was used to detect background fluorescence. Slopes were calculated from the background-subtracted data and one fusion unit is defined as 1 nmol of hydrolyzed nitrocifin per minute from 12 μg of organelle protein.

7. Ypt7 extraction assay

LEs and vacuoles isolated from BJ3505 wild type and MKY4 cells were incubated with or without 200 μM GTPγS for 10 min at 27°C prior to being added to standard fusion reactions. Samples were incubated at 27°C for 40 min, and during the last 10 min, 9.5 μM Gdi1 was added to the sample to extract Ypt7:GDP from membranes. Reactions were then immediately placed on ice, and membranes were sedimented by centrifugation. Supernatants containing Gdi extracted Rab were collected, and membrane pellets were resuspended in an equal volume of SDS sample buffer (1 M Tris-HCl pH 6.8, 10% SDS, 0.5% β-mercaptoethanol, 0.5% bromophenol blue, and 50% gylcerol). 10 μl of each sample was loaded onto a 12% SDS-PAG, electrophoresis was performed to separate proteins by size, and the presence of Ypt7 was probed by western blot analysis (see Brett et al., 2008).

8. Western Blot analysis

Sodium dodecyl sulfate (SDS)-polyacrylamide gel electrophoresis (PAGE) was performed using a Bio-Rad mini protein system (Bio-Rad Laboratories, Hercules, CA, USA). After separation, proteins were transferred onto a nitrocellulose membrane at 12 V for 8 hrs using a Royal Genie Blotter apparatus (Idea Scientific, Minneapolis, MN, USA). After blocking with 3% BSA in PBST buffer (137 mM NaCl, 2.7 mM KCl, 10 mM Na_2HPO_4, 2 mM KH_2PO_4, 0.1% Tween-20) the membranes were washed twice with PBST and incubated with primary antibody diluted to 1:1,000 in PBST for 1 hr at room temperature. The membrane was washed with PBST five times, and then incubated with FITC labeled goat anti-rabbit IgG diluted 1:10,000 in PBST for 1 hr at room

temperature. After an additional 5 washes with PBST, the membranes were probed to detect bound secondary antibody using a Typhoon fluorescence scanner (GE Healthcare, Piscataway, NJ, USA). Protein size was estimated by comparison to standard markers (Precision Plus Protein Standards, Biorad). Digital images were saved in tiff format, and processed using Adobe Photoshop CS5 software (Adobe System, San Jose, CA, USA). Brightness and contrast levels were adjusted, and an unsharpen filters were applied to the images shown.

9. Fluorescence microscopy

Yeast cells were stained with the vital dye FM4-64 to visualize vacuoles. In brief, yeast cultures were grown in SC media at 30 ^{o}C overnight and then 0.3 ml were used to inoculate a 3 ml culture in YPD media containing 3 µM FM4-64. Cells were grown for 1 hr at 30^{o}C and then washed with SC media twice, and incubated for an additional hour at 30^{o}C in 3 ml SC media. Cells were then pelleted, and resuspended in 50 µl SC media and stored at 30^{o}C until the time of imaging. Isolated LE and vacuole membranes were stained with FM4-64 by adding 5 µM FM4-64 to fusion reactions followed by incubation at 27^{o}C for 10 min for the vital dye to incorporate into the membrane. 4 µl of yeast or isolated organelles were then transferred to glass coverslip and a second glass coverslip was placed on top to sandwich the sample between glass, providing an appropriate sample thickness required for imaging. Micrographs were acquired using a Nikon Eclipse TI-E epifluorescence inverted microscope equipped with a 100 x 1.40 NA oil immersion objective lens, Photometrics EMCCD camera,

super bright LED light source, custom filter set to image separate GFP and FM4-64 channels, and NIS Element AR V4.1 software (Nikon Canada, Mississauga, ON). Digital images were saved as tiff files using Image J software (downloaded from http://rsbweb.nih.gov/ij/) and then processed using Adobe Photoshop CS5 software (Adobe System, San Jose, CA, USA). Images shown are the result of adjusting brightness and contrast levels, inverting the color, and applying an unsharpening filter.

10. Transmission Electron Microscopy

Isolated LEs and vacuoles were processed for transmission electron microscopy (TEM) using a custom protocol (Mattie, Vali & Brett, unpublished results): Fusion reactions were centrifuged at 4°C for 5 min, the supernatant was removed, 0.5 ml fixative (2.5% glutaraldehyde) was added to pellets and they were incubated overnight at 4°C. Pellets were then washed with washing buffer (0.1M sodium cacodylate) three times for 10 min and incubated in 0.5 ml freshly-prepared osmium tetroxide solution (1% OsO4 in 1.5% KFeCN) for two hours at 4 °C. Pellets were then washed with water three times for 5 min prior to dehydration by adding increasing concentration of ethanol (30%, 50%, 70%, 80%, 90%, for 10 min each, and then in 100% ethanol, 3 times for 10 min) and treatment with 100% propylene oxide twice for 5 min. For sample infiltration, pellets were incubated in 1:1 volume ratio of propylene oxide:Epon for 1 hour at room temperature. The supernatant was then replaced with 100% Epon, and samples were placed under vacuum for 1 hour to

remove bubbles and remaining traces of propylene oxide. The Samples were incubated overnight at room temperature followed by the addition of 0.5 ml fresh 100% Epon for polymerization by incubation at 57 °C for 48 hours. Epon-embedded samples were cut into 90-100 nm sections using a Ultracut microtome and DiATOME Ultra diamond knife, and each sections was then placed on a copper mesh grid. Sections on grids were stained with 4% uranyl acetate for 8 min, then with 6% lead for 5 min, and followed by three washes with water. The final samples were imaged using FEI Tecnai 120 kV electron microscope outfitted with a AMT XR80C CCD camera system at the facility for Electron Microscopy Research (McGill University, Montreal, QC). Digital images were processed using Adobe Photoshop CS5 software (Adobe Systems, San Jose, CA, USA). Brightness and contrast levels were adjusted and unsharpen filter was applied to images shown.

11. Data processing analysis

All quantitative data was processed using Microsoft Excel v.14.0.2 software (Microsoft Cooperation, Redmond, WA, USA), including calculation of mean, S.E.M., and EC_{50} values. Data was plotted using Kaleida Graph v.4.0 software (Synergy Software, Reading, PA, USA). All figures were prepared using Adobe Illustrator CS5 software (Adobe Systems, San Jose, CA, USA). The final thesis was written and assembled in Microsoft Word V14.0.2 software (Microsoft Cooperation, Redmond, WA, USA), and references were prepared using Mendeley software (Mendeley, New York, NY, USA).

Table 1. Yeast expression plasmids used in this study

Plasmids	Description	Source
pRS406	*2μ URA* (high copy, self-integrating)	Sikorski & Hieter (1989)
pRS404	*2*μ *TRP1* (high copy, self-integrating)	Sikorski & Hieter (1989)
pYJ406	pRS406 *ADHI* promoter, CPY50-Fos-ω + terminator	Jun & Wickner, 2007
pYJ406	pRS406 *ADHI* promoter, CPY50-Jun-α + terminator	Jun & Wickner, 2007
pMK001	pRS406 *ADHI* promoter, Pep12-Fos-ω + terminator	This study
pMK002	pRS404 *ADHI* promoter, Pep12-Fos-ω + terminator	This study
pMK003	pRS406 *ADHI* promoter, Pep12-Jun-α + terminator	This study
pMK004	pRS404 *ADHI* promoter, Pep12-Jun-α + terminator	This study

Table 2. Yeast strains used in this study

Strain	Genotype	Source
BJ3505	*MATα, ura3, trp1, his3, lys2, gal2, can, prb1-D1.6R, pep4::HIS3*	Jones et al., 1982
DKY6281	*MATα, leu2–3, leu2–112, ura3–52, his3-Δ200, trp1-Δ901, lys2–801*	Haas et al., 1994
MKY1	BJ3505, *ura3::NHX1-GFP:*	This study
MKY2	BJ3503, Pep12-Fos	This study
MKY3	BJ3505, Pep12-Jun	This study
BJ3505-CPY50-Fos	BJ3505, CPY50-Fos	Jun & Wickner, 2007
BJ3505-CPY50-Jun	BJ3505, CPY50-Jun	Jun & Wickner, 2007
MKY4	MKY2, *nhx1Δ::KanMX*	This study
MKY5	MKY3, *nhx1Δ::KanMX*	This study
MKY6	BJ3505-CPY50-Fos, *nhx1Δ::KanMX*	This study
MKY7	BJ3505-CPY50-Jun, *nhx1Δ::KanMX*	This study
MKY8	MKY2, *gyp6Δ::KanMX*	This study
MKY9	BJ3505-CPY50-Jun, *gyp6Δ::KanMX*	This study
MKY10	MKY4, *nhx1Δ::NatMX*	This study
MKY11	MKY7, *nhx1Δ::NatMX*	This study
MKY12	MKY10, *nhx1Δ::NatMX, gyp6Δ::KanMX*	This study
MKY13	MKY11, *nhx1Δ::NatMX, gyp6Δ::KanMX*	This study

RESULTS

1. A Novel Cell-free assay to measure late endosome vacuole fusion events

All evidence supports a model of Nhx1 function whereby it contributes to heterotypic late endosome (LE) - vacuole membrane fusion; although its role in this process is unclear, and currently there are no existing assays to study LE-vacuole fusion events. Thus, using an approach similar to that previously used to study homotypic vacuole fusion (Jun & Wickner, 2007), I designed and optimized a new LE-vacuole fusion assay that relies on the reconstitution of β-lactamase upon luminal content mixing that results from membrane fusion (Figure 3A). Membrane fractionation by sucrose gradient (Figure 3B) showed that Pep12-Fos-Gs-ω the fusion probe targeted to the LEs was found in similar fractions as resident LE proteins, e.g. Vps10. The vacuole target probe CPY50-Jun-Gs-α was found in fractions stained with vacuole resident proteins, e.g. Vps41. Importantly, the LE and vacuole probes are found in distinct fractions suggesting they are indeed targeted to separate organelles. Next, to improve organelle yield and avoid hypertonic conditions in sucrose, I isolated organelles using a 4-step ficoll gradient ,and confirmed the presence of LEs and vacuoles by western blot. By further examining this fraction by TEM, I observed both organelle populations based on morphology whereby vacuoles are spherical and have a diameter of 2 μm, whereas LEs are smaller with diameters near 400 nm (Figure 3D and E). Using fluorescence microscopy, I also demonstrate that Nhx1, our protein of interest, is found on the LEs within live cells as shown previously (Naas and Rao,

1998), and is also present on LEs proximal to vacuoles in our preparation of isolated organelles (Fig. 3F).

To quantify LE-vacuole fusion events, LEs and vacuoles were isolated by flotation on a ficoll gradient from different yeast strains harboring either Pep12-Fos-ω or CPY-Jun-α, mixed with 125 mM KCl, 5mM $MgCl_2$, and ATP, and the incubated at 27°C for 90 minutes to drive membrane fusion. Because LE-vacuole membrane fusion results in luminal content mixing, Jun and Fos proteins should bind, and the two complementary halves of β-lactamase will assemble to reconstitute activity. As shown in Figure 4A, I observed hydrolysis of nitrocefin by reconstituted β-lactamase only LE-vacuole fusion reactions that contained ATP. β-lactamase activity resulting from LE-vacuole fusion, was lower than homotypic vacuole fusion (HVF) assayed using organelles isolated from yeast expressing CPY50-Fos-ω or CPY-Jun-α (see Jun and Wickner, 2007). I then conducted a time course experiment and plotted β-lactamase activity (the slope of the lines shown in Figure 4A) to examine the kinetics of ATP-driven membrane fusion, and found that the rates of LE-vacuole and HVF were similar (Figure 4B). Together these results suggest that the new β-lactamase-based in vitro assay was indicative of LE-vacuole fusion, and was sufficiently robust (16:1 fold signal over background) to conduct further studies aimed to characterize the underlying mechanisms.

2. Ionic requirements for LE-vacuole membrane fusion

Because Nhx1 is an ion transporter that exchanges Na^+ or K^+ for H^+ across the LE membrane (see Figure 5A, Nass, 1998; Ali et al., 2004; Brett et al., 2008) and this ion

transport activity is important for its role in trafficking protein cargo between the LE and vacuole in vivo (Bowers et al., 2000; Brett et al., 2005b), I characterized the ionic requirement of LE-vacuole fusion using this new *in vitro* assay. I used HVF fusion as a benchmark because the ionic requirements of this fusion event have been previously characterized (Starai et al., 2005). Furthermore Nhx1 does not directly contributes to HVF because it is not present on vacuole membranes (Kojima et al., 2012; Nass, 1998; Bowers et al., 2000; Brett et al., 2005b), thus comparison to LE-vacuole fusion may reveal Nhx1-specific characteristics.

Because Nhx1 functions to alkalinize the lumen, opposing the activity of the V-ATPase, I first examined the effect of changing reaction buffer pH on membrane fusion (Figure 5B). As compared to HVF, LE-vacuole fusion was less tolerant to changes in pH with maximal fusion signal observed between pH 6.7 and pH 6.8. Because K^+ is transported by Nhx1, I examined the effect of increasing KCl in the reaction buffer (Figure 5C). Like pH, LE-vacuole fusion is less tolerant to shifts of KCl than HVF. Replacing K^+ with either Na^+ or NH_4^+ had similar effects on HVF and LE-vacuole fusion, although NH_4^+ only partially replaced K^+ activity (Figure 5D). However, LE-vacuole fusion was more tolerant to Rb^+ than HVF, suggesting the presence of a Rb^+ transporting mechanism on the LE that is not present on the vacuole. Replacing Cl^- with acetate has been shown to impair HVF at the cost of promoting vacuole fission (Michaillat et al., 2012). Furthermore, addition of acetate to yeast cells disrupts endocytosis in a manner that implies inhibition of LE-vacuole fusion (Brett et al., 2005b). However, KoAc has no effect on LE-vacuole fusion *in vitro* (Figure 5D).

It has been proposed that Nhx1 may contribute to LE volume regulation by coordinating function with Gef1, a Cl^- channel, to import KCl into the lumen, which in turn promotes H_2O influx through an aquaporin (likely Fps1; Nass, 1998) by osmosis (Figure 5A). To confirm that anion transport was present and contribute to fusion, I tested whether addition of DIDS (4,4'-Diisothiocyanatostilbene-2,2'-disulfonic acid) a chemical inhibitor of anion channels, impaired LE-vacuole fusion (Figure 5E). Addition of increasing concentrations of DIDS blocked LE-vacuole and HVF, with a maximal effect of inhibition observed in the presence of 5 μM for HVF and 8 μM for LE-vacuole fusion, suggesting that anion transporter function may contribute to membrane fusion events. HVF has been shown to be enhanced with hypotonic shock (0.1 M sorbitol) and impaired by hypertonic shock (≥ 0.5 M sorbitol) as a result of osmosis (Brett and Merz, 2008). LE-vacuole fusion, however, is not affected by hypotonic treatment, although hypertonic shock has a greater effect at 0.5 M than that observed for HVF (Figure 5F).

Finally, because the H^+ electrochemical gradient across the vacuole membrane is important for Ca^{2+} loading into the lumen of the vacuole by Vcx1 (a Vacuolar membrane antiporter with Ca^{2+}/H^+ activity; Cunningham and Fink, 1996) and Ca^{2+} efflux is necessary for HVF at a late stage (Merz and Wickner, 2004), I examined the effects of $CaCl_2$ addition on membrane fusion. Consistent with earlier findings (Bayer et al., 2003), HVF is first impaired (1 mM) but then recovers with increasing concentrations of $CaCl_2$ (10 mM; Figure 6A). However, the inhibitory effect at 1 mM was less for LE-vacuole fusion, and fusion is stimulated at 10 mM $CaCl_2$ relative to HVF. Consistent with this result, is the observation that LE-vacuole fusion was more

sensitive to EGTA, a divalent cation chelator with preference for Ca^{2+} over Mg^{2+} (dissociation constant pK = 10.9 μM for Ca^{2+}, and 5.4 μM for Mg^{2+}; Orlov et al., 1985; Figure 6B). LE-vacuole fusion is also sensitive to EDTA, a divalent cation chelator with higher affinity to Mg^{2+} over Ca^{2+} (pK = 8.7 μM for Ca^{2+}, and 10.8 μM for Mg^{2+}; Orlov et al., 1985 ; Figure 6B) suggesting that Mg^{2+} is also important for fusion, as it is necessary to coordinate nucleotide binding and hydrolysis by ATPases (like Sec18) and GTPases (Ypt7) involved in this process (Starai et al., 2005).

In summary, LE-vacuole fusion has different ionic requirements than HVF: it was less tolerant to changes in pH or KCl, but can tolerate Rb^{+} replacement of K^{+} and acetate replacement of Cl^{-}. It was not affected by a hypotonic shock but was more sensitive than HVF to hypertonic shock, and was hypersensitive to EGTA and can be stimulated by 10 mM $CaCl_2$. These data suggest that a different complement of ion transporters regulate each fusion event and that the observed ionic profile for LE-vacuole fusion is indicative of Nhx1 function at the late endosome.

3. Protein machinery required for late endosome-vacuole membrane fusion

Homotypic vacuole fusion requires action of various proteins, enzymes and lipids to drive progressive subreactions required for bilayer lipid mixing (see Figure 2). Based on genetic studies and analysis of endocytic trafficking *in vivo*, it is thought that many of these proteins also drive LE-vacuole fusion, which is not surprising as both events involve the vacuole membrane (Balderhaar et al., 2010). However, prior to my studies there was no *in vitro* assay to definitely test this hypothesis. Thus, I

characterized the proteins required for this fusion event using the new LE-vacuole fusion assay I develped. ``Priming`` the first stage of HVF requires Sec17, a SNARE chaperone, and blocking Sec17 with a specific antibody inhibits HVF (Figure 7A). Because Sec17 is the only SNARE chaperone encoded in the *S. cerevisiae* genome that is thought to contribute to membrane fusion at many sites within the cell (Schwartz and Merz, 2009), it is not surprising that anti Sec17 antibody also blocks LE-vacuole fusion, suggesting a role in this process.

The ``tethering`` subreaction of HVF requires active Rab-GTPases (Lachmann et al., 2011). Addition of Gdi1, a Rab-GTPase chaperone protein that extracts inactive Rabs from membranes, or purified Gyp1-46 protein, the catalytic domain of Gyp1, a Rab-GAP protein, capable of inactivating most Rabs, block both fusion events, suggesting that Rab-GTPase function is required for LE-vacuole fusion like HVF. Specifically the Rab-GTPase Ypt7 is known to drive HVF (Wang et al., 2003a) and has been implicated in LE-vacuole fusion based on work that manipulated cellular Ypt7 expression levels to alter delivery of protein cargos from the LE to vacuole *in vivo* (Balderhaar et al., 2010). Indeed, an affinity purified antibody to Ypt7 blocks both fusion events, whereas an antibody to Vps21, the Rab responsible for early endosome fusion and LE maturation has no effect, confirming the enrolment of Ypt7 in both reactions (Figure 7A).

Next, the ''docking'' subreaction requires Vps33, a SM-protein ortholog and component of the HOPS holocomplex that coordinates Rab signalling and SNARE assembly necessary for HVF. All 6 subunits of HOPS including Vps33 localize to the LE

as well as vacuole suggesting that it mediates heterotypic membrane fusion between the LE and vacuole (Balderhaar and Ungermann, 2013). This was confirmed as affinity purified anti Vps33 antibody blocked both fusion events.

The final ''fusion'' subreaction of HVF requires the activities of SNARE proteins (Ungermann et al., 1999). The vacuole ortholog of syntaxin Vam3, a Q-SNARE, interacts with the synaptobrevin ortholog Nyv1, a R-SNARE, across membranes and form a 4 helix bundle complex in trans with Vam7, the yeast SNAP25 ortholog (Ungermann and Wickner, 1998). On the LE, Vam3 is replaced by Pep12, the LE specific syntaxin ortholog (Becherer et al., 1996). Addition of an antibody against Vam3 block HVF, as predicted, and LE-vacuole fusion (Figure 7A). Whereas, an antibody against Pep12 only impaired LE-vacuole fusion. This result is important because it demonstrates that both LE and vacuole syntaxin orthologs contribute to LE-vacuole fusion.

Finally, addition of purified recombinant Vam7 protein, a soluble Q-SNARE, drives HVF in the absence of ATP, a process called ''bypass fusion'' because it bypasses the need for priming by Sec17 and tethering by Rab-GTPases (Stroupe et al., 2006). When the chaperone activity of Sec17 is blocked by an antibody, excess Vam7 can further stimulate SNARE driven membrane fusion, because it has improved access to Vam3 and Nyv1, allowing formation of more SNARE complexes (Thorngren et al., 2004). Because Vam7 is the only soluble Q-SNARE though to function in the endocytic pathway (Ungermann and Wickner, 1998; Stroupe et al., 2006; Jun and Wickner, 2007; Collins and Wickner, 2007), addition of purified recombinant Vam7 protein

stimulates heterotypic LE-vacuole fusion, like HVF (Figure 7B). As previously reported for HVF (Thorngren et al., 2004), addition of ATP to the bypass fusion reaction has a mild inhibitory effect on LE-vacuole fusion as well, presumably due to an ATP-dependent activity that prevents the SNARE-mediated bypass mechanism (trans SNARE complex proof-reading by hops; Stroupe et al., 2006). However, one striking distinction between these two fusion events, is that LE-vacuole bypass fusion is not enhanced by Sec17 block, suggesting that a different mechanism may drive SNARE function at LEs.

4. H^+-transport by Nhx1 contributes to LE - vacuole fusion

To determine if Nhx1 contributes to LE–vacuole fusion, I knocked out NHX1 in yeast strains harbouring different fusion probes, isolated their LEs and vacuoles and examined their ability to fuse in vitro. As hypothesized, knocking out NHX1 causes impairment in LE-vacuole fusion (57 % less than WT at 90 min; Figure. 8A). To test whether the loss of H^+-transport by Nhx1 underlies the observed effect, I first measured LE–vacuole fusion over a range of pH values between 6.2 and 7.3 (Figure 8B). Deleting NHX1 shifted the pH-sensitivity of the LE–vacuole fusion reaction to the right, suggesting that fusion is hypersensitive to low pH and hyper resistant to high pH. Similarly, knocking out NHX1 rendered heterotypic fusion hypersensitive to acetate, a weak acid (Figure 8C). Consistent with both observations, I found that impairment of LE–vacuole fusion is suppressed by adding increasing concentrations of chloroquine, a weak base that is known to accumulate in the lumen of acidic

organelles to raise pH (Wattiaux et al., 2000; Figure 8D). These results are consistent with earlier findings showing that hyperacidity caused by deleting NHX1 underlies the endocytic trafficking defects in intact cells (Brett et al., 2005b). Finally, because Nhx1 is an obligate exchanger and is the only known transporter on the LE known to transport Rb^+ (in place of Na^+; Nass, 1997; Brett et al., 2005b), I next determined if replacing K^+ with Rb^+ or other monovalent cations affected LE–vacuole fusion in the absence of NHX1 (Figure 8C). Unlike Na^+ or NH_4^+, heterotypic fusion was not tolerant to Rb^+ in the absence of NHX1. Together these results suggest that monovalent cation/H^+ transport by Nhx1 is required for LE-vacuole fusion.

5. Vam7 suppresses fusion defects caused by *nhx1*Δ

Having shown that Vam7 can drive LE - vacuole fusion, I sought to determine whether addition of Vam7 bypasses the fusion reaction affected by knocking out NHX1 (Figure 9). Bypass fusion by simple addition of purified recombinant Vam7 to fusion reactions in the presence or absence of ATP had minor effects on the fusion impairment caused by deleting NHX1. However, pre-treating the organelles with anti-Sec17 antibody to further enhance Vam7 mediated SNARE-pairing and fusion (Jun & Wickner, 2007), completely suppressed the *nhx1*Δ phenotype. This result suggests that knocking out Nhx1 impairs a stage of the fusion reaction that can be bypassed by Vam7-mediated fusion.

6. The Nhx1-Gyp6 interaction does not mediate LE - vacuole fusion

Nhx1 binds Gyp6, a Rab-GAP that inactivates Ypt7 *in vitro* and knocking out GYP6 suppresses some trafficking defects caused by deletion of NHX1 in intact cells (Ali et al., 2004; Will and Gallwitz, 2001). As loss of GYP6 would increase baseline Ypt7 activity, I hypothesize that GYP6 deletion may suppress heterotypic fusion defects observed in absence of NHX1. To test this hypothesis, I knocked out GYP6 from WT and nhx1Δ cells containing complementary fusion probes and examine the effect on *in vitro* LE-vacuole fusion (Figure 10A). Surprisingly, heterotypic fusion was not affected by GYP6 deletion, in the absence or presence of NHX1. Addition of the Rab chaperone Gdi1 to the fusion reaction will extract inactive Rab from membranes and block fusion. If more active Rab:GTP is found on the membrane, less Rab is extracted and fusion is resistant to Gdi1 (see Brett et al., 2008). Thus, I tested whether the sensitivity of LE – vacuole fusion to Gdi1 was affected by deleting GYP6 (Figure 10B). Again, knocking out GYP6 did not change sensitivity of the reaction to Gdi1 in any of strains tested (Figure. 10B), suggesting that Gyp6 does not regulate LE – vacuole fusion.

Although these results rule out a potential role for Gyp6 in LE–vacuole fusion, it is possible that Nhx1 may interact with another Rab-GAP to stimulate Ypt7 and drive fusion. To test this hypothesis, I determined whether deleting NHX1 changes the sensitivity of the fusion reaction to Gyp1-46, the N-terminal fragment of Gyp1 that only contains the catalytic TBC domain responsible for Rab inactivation, which is known to inactivate Ypt7 and block homotypic vacuole fusion in vitro (Wang et al., 2003b). As shown in Figure 10C, knocking out NHX1 does not change the sensitivity

of the LE- vacuole fusion reaction to Gyp1-46. Together, these results omit a role for Gyp6 GAP activity in LE-vacuole fusion, and thus suggest that the Nhx1-Gyp6 interaction is not important for LE-vacuole fusion.

7. Ypt7 Rab activation is not impaired by the loss of NHX1

To strengthen my previous findings whereby Nhx1-Gyp6 interaction is not important for LE-vacuole fusion, I tested the relative amount of inactive Ypt7 on LE and vacuole membranes by treating isolated organelles with recombinant Gdi1, the Rab chaperone protein that preferentially extracts inactive Rab-GDP from membranes. Otherwise Rab-proteins are anchored to the membrane by two covalently linked geranyl-geranyl groups, and thus cannot freely dissociate (Hutagalung & Novick, 2011). I separated the soluble Gdi1-bound Ypt7:GDP from membrane bound Ypt7:GTP by centrifugation and determined the relative amounts of each by western blot analysis. As controls, I added the non-hydrolyzable GTP analog GTPγS to the reaction, which binds to Rabs on the surface and activates them, preventing extraction by Gdi1, or I added a recombinant Rab-GAP protein (Gyp1-46) to drive GTP hydrolysis and promote extraction (Figure 11). As expected, and consistent with the previous observations from LE-vacuole fusion (see Figure 10C), no significant difference in the relative amounts of inactive Ypt7 (Ypt7:GDP) between WT and *nhx1Δ* was detected, suggesting that Nhx1 does not regulate Ypt7 signaling to regulate LE-vacuole fusion.

Figure 3. Cell-free LE-vacuole membrane fusion

(A) A new in vitro assay to quantify LE-vacuole fusion, homotypic vacuole fusion, and homotypic LE fusion. (B) Western blot analysis of yeast membranes separated by a sucrose gradient indicate that the fusion probes are properly localized to vacuole (blue) and/or LE (yellow), based on the location of vacuole marker Vps41 or LE marker Vps10. Fractions collected from either cells expressing CPY50-Fos- ω or Pep12-Fos- ω are shown. (C) Transmission electron micrographs indicate that our organelle preparation using the ficoll method contains vacuoles and LEs based on size and morphology, and that they make contact in vitro: vacuole-vacuole (blue), LE-vacuole (green), and LE-LE (red) interactions are highlighted in boxes. (D) Western blot analysis of organelles isolated using the ficoll method indicates that both LE- and vacuole- specific protein markers are present. Fractions collected from either cells expressing CPY50-Jun-α or Pep12-Fos-ω are shown. (E) Fluorescence micrographs of organelles isolated using the ficoll method (right panel) or intact cells (left panel) expressing Nhx1-GFP. Vacuoles were stained with FM4-64 and Nhx1-GFP has previously been shown to reside on LEs (Nass & Rao, 1997; Bowers et al., 2000; Brett et al., 2005).

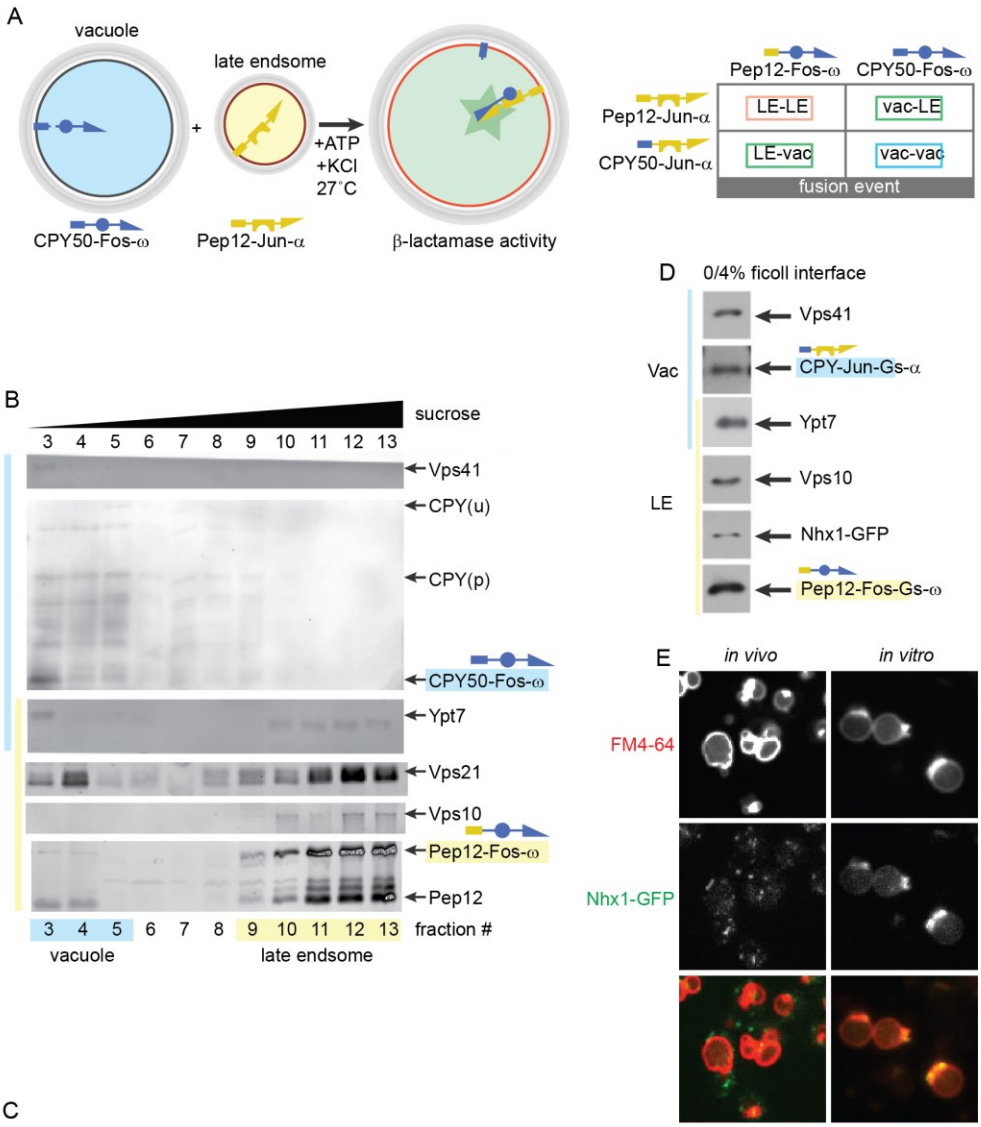
A
vacuole
late endsome
+ATP
+KCl
27˚C
CPY50-Fos-ω
Pep12-Jun-α
β-lactamase activity
Pep12-Fos-ω
CPY50-Fos-ω
Pep12-Jun-α
CPY50-Jun-α
LE-LE
vac-LE
LE-vac
vac-vac
fusion event
B
sucrose
3 4 5 6 7 8 9 10 11 12 13
Vps41
CPY(u)
CPY(p)
CPY50-Fos-ω
Ypt7
Vps21
Vps10
Pep12-Fos-ω
Pep12
3 4 5 6 7 8 9 10 11 12 13 fraction #
vacuole
late endsome
D
0/4% ficoll interface
Vps41
Vac
CPY-Jun-Gs-α
Ypt7
Vps10
LE
Nhx1-GFP
Pep12-Fos-Gs-ω
E
in vivo
in vitro
FM4-64
Nhx1-GFP
C
2 μm
1 μm

Figure 4. Reconstituted β-lactamase activity and membrane fusion

(A) Rate of hydrolysis of nitrocefin by β-lactamase reconstituted upon lumenal mixing as a result of membrane fusion. Organelles isolated by ficoll gradient from strains expressing either vacuole-localized CPY50-Fos-ω or CPY50-Jun-α probes (Vac-Vac) or strains expressing vacuole-localized CPY50-Fos-ω or LE-localized Pep12-Jun-α probes (LE-Vac) were mixed in the presence or absence of ATP in presence of fusion reaction buffer and incubated for 90 minutes at 27˚C. (B) LE-vacuole or homotypoic vacuole fusion was monitored over 90 minutes in the presence or absence of ATP. At t = 0 minutes, reactions were incubated at 27˚C and then removed, placed on ice at the time points shown, and β-lacatamase activity was measured as shown in A. Mean ± S.E.M. values are plotted and at least 3 experiments were performed for each condition shown.

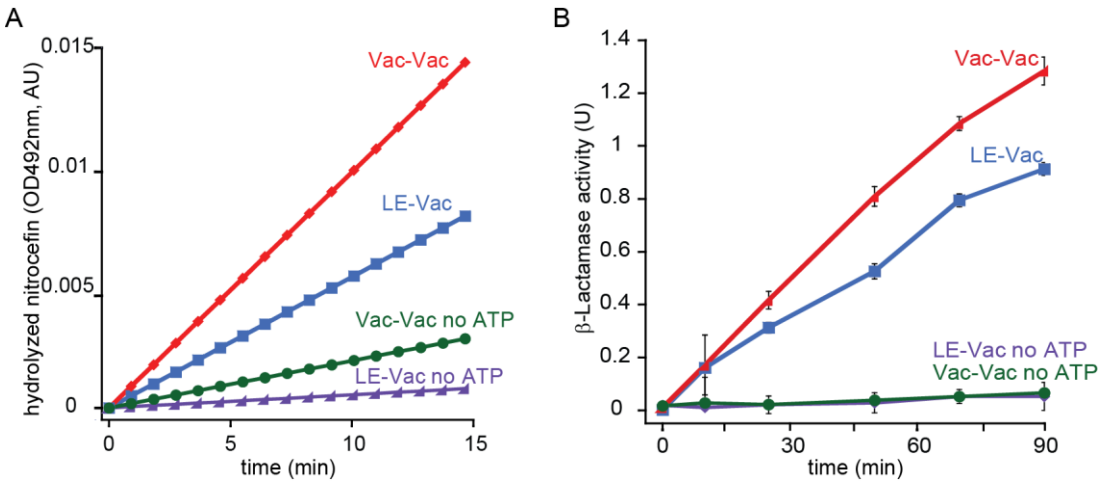
A
0.015
0.01
0.005
0
hydrolyzed nitrocefin (OD492nm, AU)
Vac-Vac
LE-Vac
Vac-Vac no ATP
LE-Vac no ATP
0
5
10
15
time (min)
B
1.4
1.2
1
0.8
0.6
0.4
0.2
0
β-Lactamase activity (U)
Vac-Vac
LE-Vac
LE-Vac no ATP
Vac-Vac no ATP
0
30
60
90
time (min)

Figure 5. Ionic effects on LE-vacuole fusion

(A) Model of ion transporters function at the LE. Nhx1 and Gef1 use the H^+ electrochemical gradient created by the V-ATPase to import K^+ or Cl^-, respectively. Net KCl import would create an osmotic gradient causing water influx through an aquaporin to increase organelle volume. LE-vacuole fusion or HVF was measured in the presence of increasing pH (B) or KCl (C), or when replacing KCl with other salts (D) in the reaction buffer. Similarly, the effects of adding increasing amounts of DIDS (E) or changing the amount of sorbitol in the reaction to induce osmosis (G) on LE-vacuole or HVF were also examined. All fusion reactions were incubated for 90 minutes at 27˚C in the presence of ATP. Asterisks denote standard fusion reaction conditions. Mean ± S.E.M. values are plotted and $n \geq 3$ for all conditions shown.

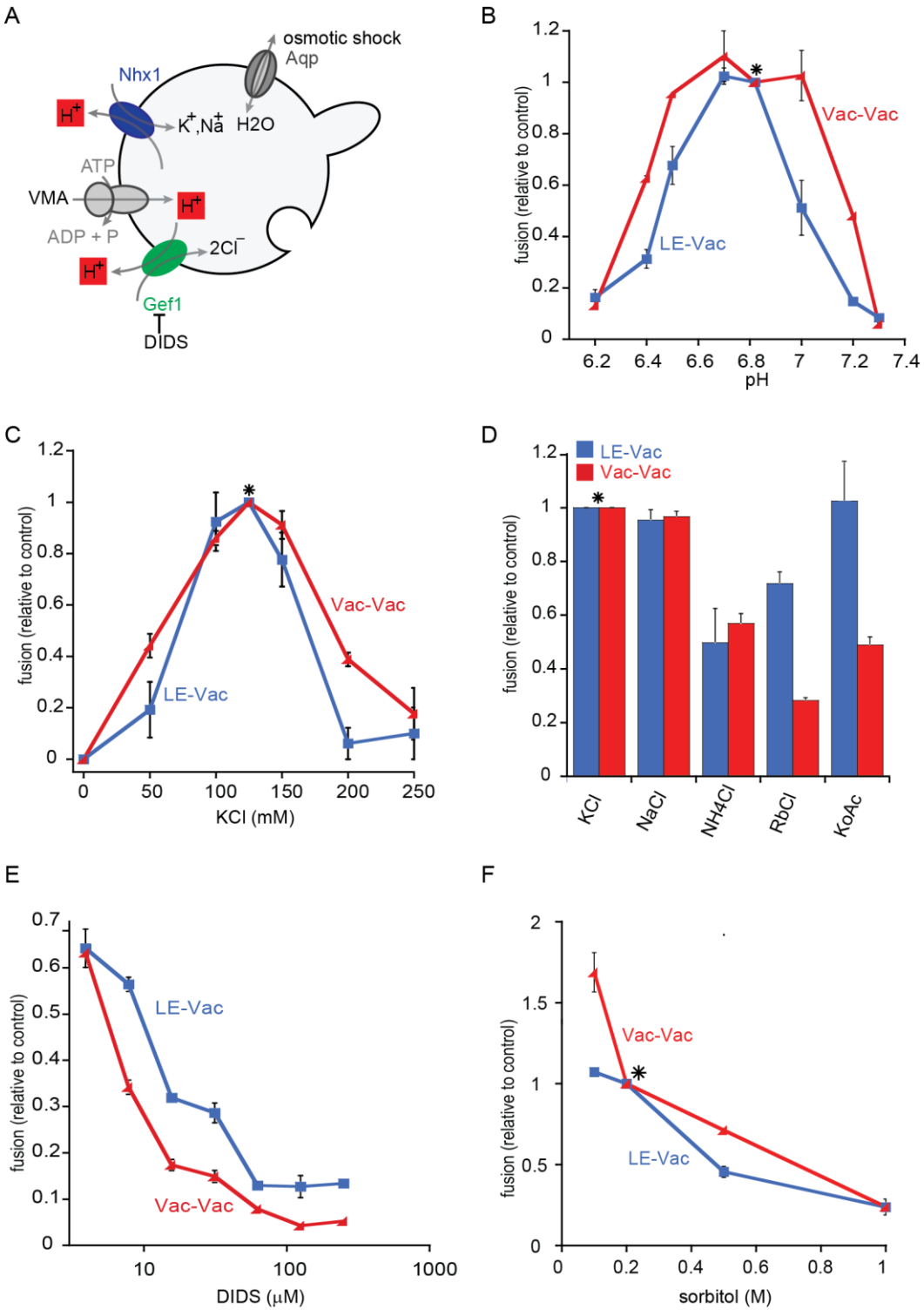
A
osmotic shock
Aqp
Nhx1
H+
K+,Na+
H2O
ATP
VMA
H+
ADP + P
2Cl−
H+
Gef1
DIDS
B
fusion (relative to control)
pH
Vac-Vac
LE-Vac
C
fusion (relative to control)
KCl (mM)
Vac-Vac
LE-Vac
D
LE-Vac
Vac-Vac
fusion (relative to control)
KCl
NaCl
NH4Cl
RbCl
KoAc
E
fusion (relative to control)
DIDS (μM)
LE-Vac
Vac-Vac
F
fusion (relative to control)
sorbitol (M)
Vac-Vac
LE-Vac

Figure 6. Effect of divalent cations on LE-vacuole fusion

In vitro LE-vacuole or homotypic vacuole fusion was measured in the presence of increasing concentrations of $CaCl_2$ (A), or the divalent cation chelators EGTA or EDTA (B). All fusion reactions were incubated for 90 minutes at 27˚C in the presence of ATP. Asterisks denote standard fusion reaction conditions. Mean ± S.E.M. values are plotted and $n \geq 3$ for all conditions shown.

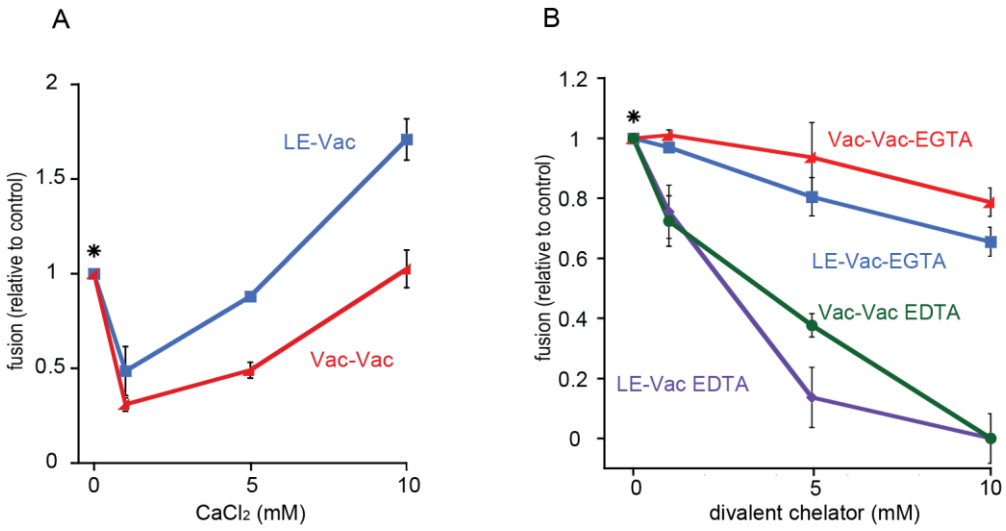
A
B
fusion (relative to control)
CaCl2 (mM)
LE-Vac
Vac-Vac
divalent chelator (mM)
Vac-Vac-EGTA
LE-Vac-EGTA
Vac-Vac EDTA
LE-Vac EDTA

Figure 7. Characterization of proteins that regulate LE-vacuole fusion

(A) Like homotypic vacuole fusion (blue bars), LE-vacuole fusion (red bars) is sensitive to affinity-purified antibodies against Sec17 (1.8 μM), Ypt7 (1.8 μM), Vps21 (1.2 μM), Vps33 (1.8 μM), Vam3 (2.6 μM), and purified recombinant Gdi1 (1.0 μM) and Gyp1-46 (2.0 μM) proteins. However unlike LE-vacuole fusion, homotypic vacuole fusion was not sensitive to affinity-purified anti-Pep12 antibody (1.2 μM). The stage of the membrane fusion reaction associated with each protein is indicated below. (B) Purified recombinant Vam7 protein (100 nM) promoted bypass fusion in absence of ATP. Vam7 bypass fusion was also performed in the presence of ATP, or after preincubation of organelles with 1.8 μM anti-Sec17 to reveal more SNARE proteins (Thorngren et al., 2004). All reactions were incubated for 90 min at 27˚C with the exception of negative controls that were kept on ice, to prevent fusion. Asterisks denote standard fusion reaction conditions. Mean ± S.E.M. values are plotted and $n \geq 2$ for all conditions shown.

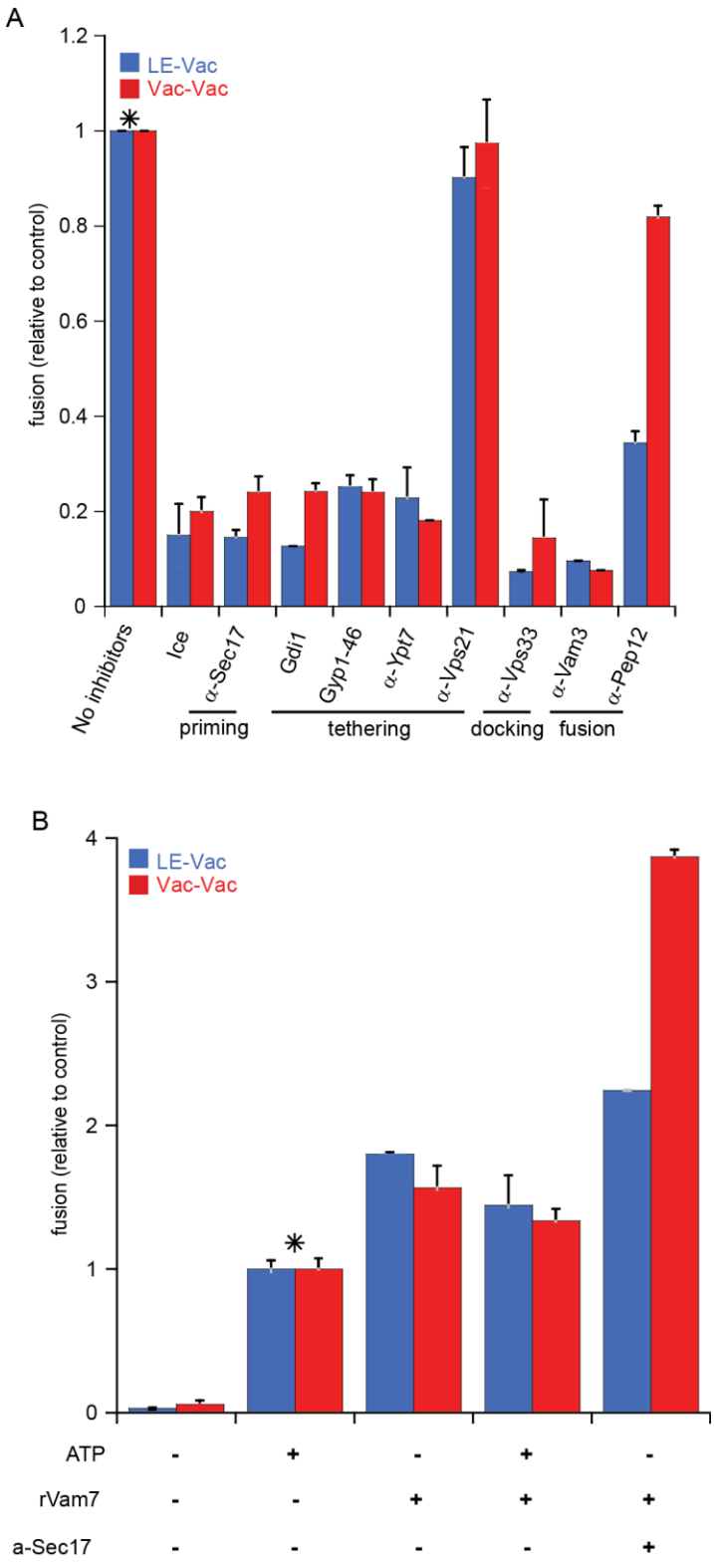
A
LE-Vac
Vac-Vac
fusion (relative to control)
1.2
1
0.8
0.6
0.4
0.2
0
No inhibitors
Ice
α-Sec17
Gdi1
Gyp1-46
α-Ypt7
α-Vps21
α-Vps33
α-Vam3
α-Pep12
priming
tethering
docking
fusion
B
LE-Vac
Vac-Vac
fusion (relative to control)
4
3
2
1
0
ATP - + - + -
rVam7 - - + + +
a-Sec17 - - - - +

Figure 8. Ion transport by Nhx1 drives LE-vacuole fusion

(A) In vitro LE–vacuole fusion in the absence (red) or presence (blue) of NHX1 was measured over time (A), over a range of pH values (B), when KCl was replaced with different salts (125 mM, C) or in the presence of increasing concentrations of chloroquine (D). All reactions were incubated in the presence of ATP for 90 min at 27˚C with the exception of the time-course data shown in A. Fusion values shown are means (± S.E.M.) normalized to standard fusion conditions in B and C or the value obtained for organelles isolated from wild type cells under fusion conditions (A and D). Asterisks denote standard fusion reaction conditions. $n \geq 3$ for all conditions shown.

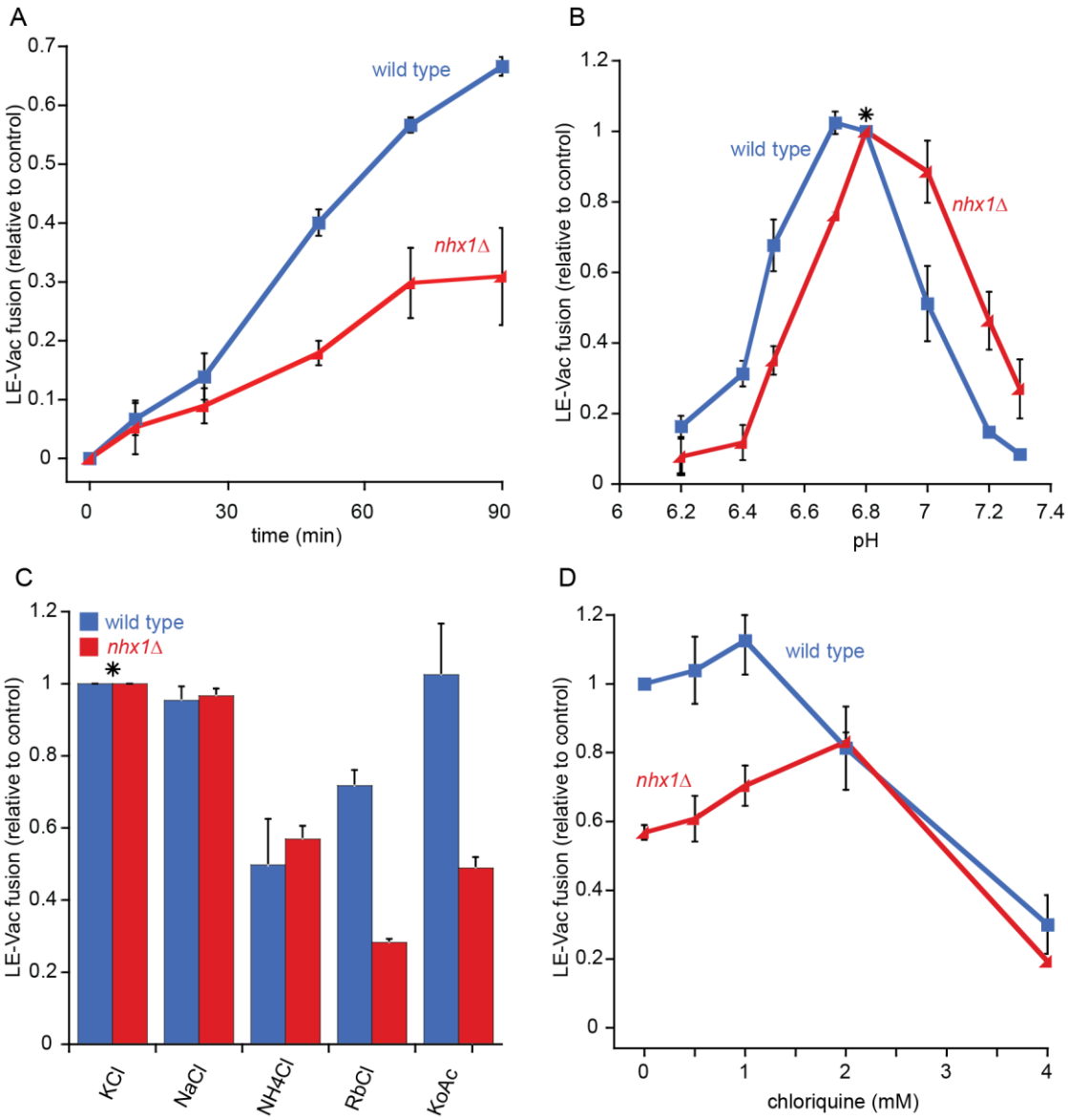
A
LE-Vac fusion (relative to control)
time (min)
wild type
nhx1Δ
B
LE-Vac fusion (relative to control)
pH
wild type
nhx1Δ
C
LE-Vac fusion (relative to control)
wild type
nhx1Δ
KCl
NaCl
NH4Cl
RbCl
KoAc
D
LE-Vac fusion (relative to control)
chloriquine (mM)
wild type
nhx1Δ

Figure 9. Vam7 bypass fusion suppresses the *nhx1*Δ phenotype

Purified recombinant Vam7 protein (100 nM) marginally improved heterotypic fusion of organelles isolated from nhx1Δ cells (red bars) as compared to wild type (blue bars), in the absence and presence of ATP. But after pre-incubating organelles with 1.8 μM anti-Sec17 for 20 minutes at 27˚C, addition of Vam7 completely suppressed fusion defects caused by deleting NHX1. Reactions without Vam7 and ATP, or with ATP are shown as negative and positive controls respectively. Fusion values shown were normalized to the standard, ATP-driven wild type condition (*). Mean ± S.E.M. values are plotted and $n \geq 2$ for all conditions shown.

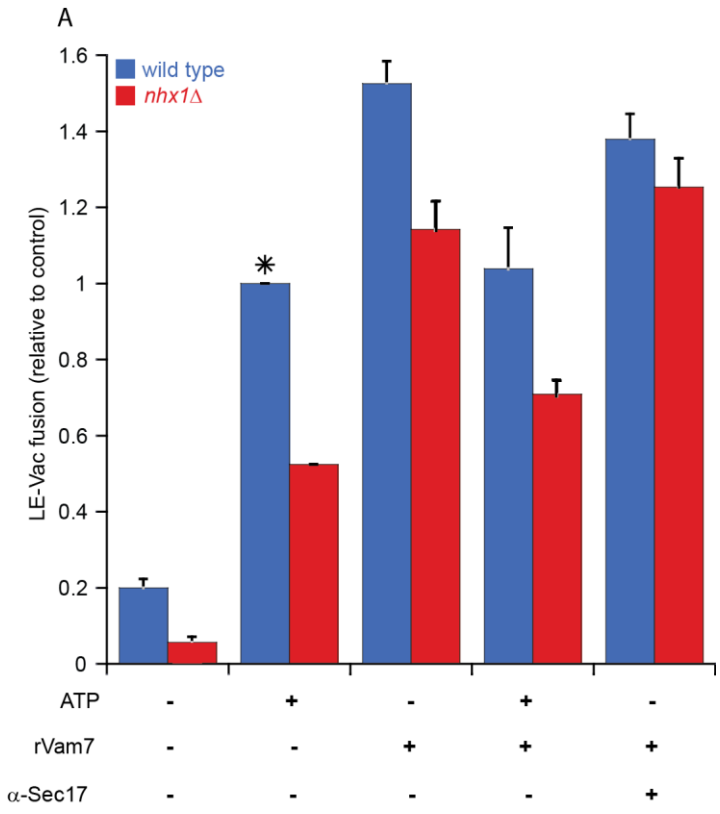
A
wild type
nhx1Δ
LE-Vac fusion (relative to control)
1.6
1.4
1.2
1
0.8
0.6
0.4
0.2
0
*
ATP - + - + -
rVam7 - - + + +
α-Sec17 - - - - +

Figure 10. Knocking out GYP6 has no effect on LE–vacuole fusion

(A) In vitro LE-vacuole fusion using organelles isolated from wild type (blue), *nhx1Δ* (red), *gyp6Δ* (purple), or *nhx1Δgyp6Δ* (green) cells was measured over 90 minutes, or at 90 minutes in the presence of increasing concentrations of recombinant purified Gdi1 protein (B) or Gyp1-46 protein (C). EC_{50} values are also shown in panel B. Data was normalized to fusion of wild type organelles under standard fusion conditions (i.e. no inhibitors, 90 minutes). All reactions were incubated in the presence of ATP. Mean ± S.E.M. values are plotted and $n \geq 2$ for all conditions shown.

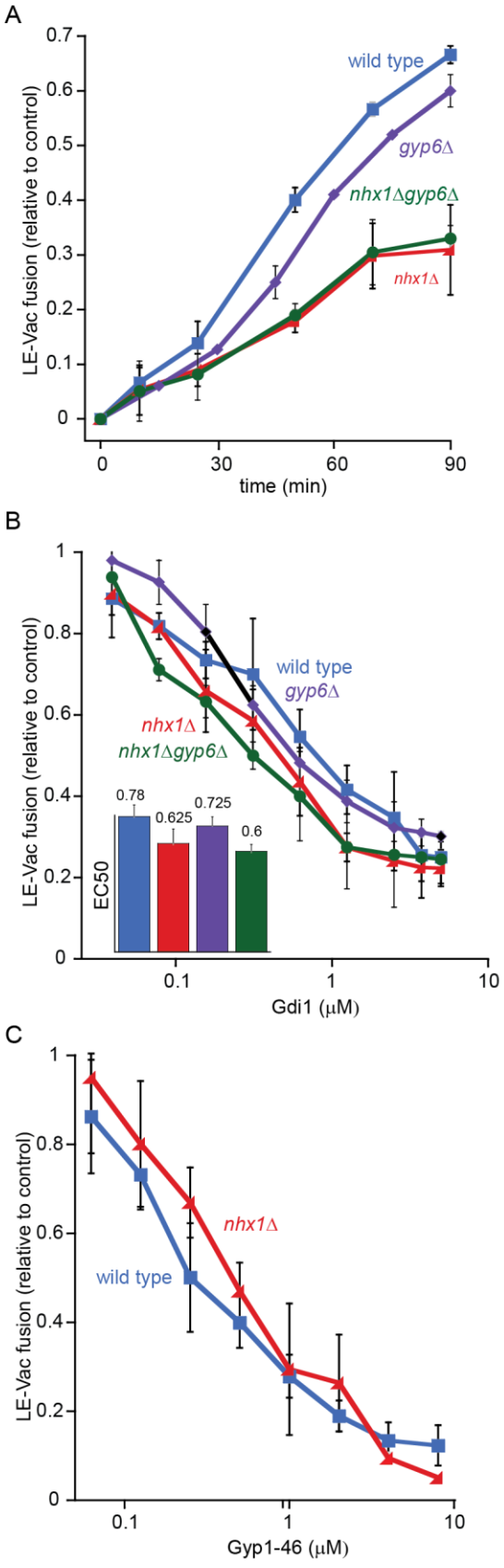
A
LE-Vac fusion (relative to control)
time (min)
wild type
gyp6Δ
nhx1Δgyp6Δ
nhx1Δ
B
LE-Vac fusion (relative to control)
Gdi1 (μM)
wild type
gyp6Δ
nhx1Δ
nhx1Δgyp6Δ
EC50
0.78
0.625
0.725
0.6
C
LE-Vac fusion (relative to control)
Gyp1-46 (μM)
nhx1Δ
wild type

Figure 11. Deletion of NHX1 does not cause Ypt7 inactivation

In vitro LE-vacuole fusion reactions were incubated for 30 minutes at 27˚C in the presence of ATP and then treated with 5 μM purified recombinant Gdi1 protein for 10 minutes to extract only Ypt7:GDP from membranes. Reaction buffer was used in place of Gdi1 as a negative control. In addition, vacuoles were pretreated with either 5 μM Gyp1-46 protein or 200 μM GTPγS prior to Gdi1 addition, to further inactivate or prevent inactivation of Ypt7 respectively. The relative amount of Ypt7 extracted by Gdi1 (supernatant) compared to Ypt7 bound to membrane (pellet) is shown for each condition by western blot analysis. Ypt7:GDP extraction by Gdi1 from membranes isolated from nhx1Δ cells is not significantly different than that observed from wild type membranes. $n \geq 2$ for all conditions shown.

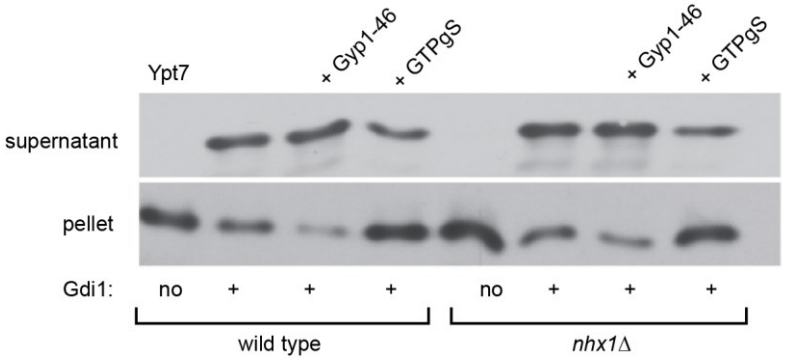
Ypt7
+ Gyp1-46
+ GTPgS
+ Gyp1-46
+ GTPgS
supernatant
pellet
Gdi1:
no
+
+
+
no
+
+
+
wild type
nhx1Δ

DISCUSSION

1. A new assay for late endosome-vacuole fusion in vitro

Compared to previously published cell-free assays and fluorescence microscopy-based assays of organelle fusion, the advantages of this particular method are numerous: (1) It is not reliant on fluorescence microscopy, which cannot accurately resolve late endosome fusion events because the size of these organelles (about 400 nm) is near the spatial resolution limitation of light microscopy (Barysch et al., 2010). (2) It is quantitative and robust, as it gives a 16:1 signal to noise ratio, which is significantly higher than previously reported cell-free assays of organelle fusion (Abazeed et al., 2005), allowing us to detect relatively small changes in fusion. (3) We speculate that this assay is robust because we only use freshly prepared organelles, unlike protocols that employ frozen organelle preparations (Barysch et al., 2010), as freezing causes formation of water ice crystals that will rupture organelles. (4) To circumvent lysis caused by freezing or to purify organelles, many researchers store or isolate organelles in buffers with high osmolarity or viscosity. But we've shown that these conditions impair membrane fusion, and took precautions to isolate organelles using a ficoll gradient that permits LE and vacuole isolation in a buffer that has similar osmolarity to the yeast cytoplasm. (5) Rather than having to exclusively rely on genetic approaches to study this fusion event, our *in vitro* assay allows us to add chemical and protein inhibitors or recombinant proteins to the cytoplasmic face of isolated organelles, so that we may directly test their effects on the fusion machinery (e.g. Wickner, 2010). (6) The amount of material required for these assays is not limiting, as isolating organelles from six 1 L yeast cultures yields sufficient late

endosomes and vacuoles to conduct approximately 100 fusion reactions. However, I suspect that we can improve upon this first iteration of the assay by re-engineering the probes to improve β-lactamase assembly in the lumen of fusion products by exchanging c-Fos and Jun (K_d = 110 nM) with smaller, higher-affinity binding partners, e.g. MP1 and p14 (K_d = 12.8 nM). Furthermore, other organelle purification techniques should be tested, e.g. an OptiPrep gradient, to separate the two organelle populations. This is necessary to better understand the stoichiometry of the heterotypic fusion reaction, and will limit fusion events to only organelles containing probes.

2. Protein machinery required for LE-vacuole fusion

Our LE-vacuole fusion results support a model of LE-vacuole fusion presented by Christian Ungermann's group, that is based entirely on genetics and *in vivo* trafficking assays, whereby they either deleted or overexpressed genes encoding proteins hypothesized to contribute to LE-vacuole fusion (Rabs Ypt7 or Vps21, tethering complexes HOPS or CORVET subunits, SNAREs, ESCRT subunits, GEFs and GAPs) and then examine the effects on protein cargo trafficking from the LE to vacuole and late endosome or vacuole morphology *in vivo*. Herein, we provided definitive evidence that SANRE chaperone Sec17, component of HOPS tethering complex Vps33, the Rab-GTPase Ypt7, and the SNAREs Vam7 and Vam3 are shared for homotypic vacuole and LE-vacuole fusion. However, these findings are not surprising as both fusion events involve the vacuole membrane. We also determined that Pep12, a homolog of the syntaxin Vam3 found on the LE, is only required for LE-vacuole fusion. This result is

consistent with the observation that Pep12 can form a complex with vacuolar SNAREs Vti1 and Vam7, which then interacts with the R-SNARE Nyv1 to form a functional trans-SNARE complex that drives fusion of liposomes. Importantly, liposome fusion driven by this complex is less efficient than by a complex entirely made up of vacuole SANREs (by replacing Pep12 with Vam3), which mirrors our in vitro fusion results (Fig. 4B; see Izawa et al., 2012). These results suggest that SNARE complex formation with Pep12 is not as efficient as with Vam3.

Additional studies are needed to Vps41 (specific for HOPS) and Vps8 (specific for CORVET) to further understand what specific subunits of the tethering complex (VpsC) are involved in membrane fusion at the endosome and with what other organelles.

We also demonstrate that LE-fusion can be stimulated in vitro by the addition of ATP, presumably by initiating the Sec18-mediated priming reaction. However, addition of excess purified Vam7 protein bypassed the need for ATP to drive LE-vacuole fusion, On the other hand, LE-vacuole fusion was only rescued in *nhx1Δ* when priming was blocked with anti Sec17. These results suggest that the mechanism by which SNAREs drive membranes to fuse is different between LE-vacuole and HVF, and that Nhx1 and Sec17 might function together to initiate the early stages of fusion.

3. Ion exchange by Nhx1 drives LE-vacuole fusion

Within intact cells, Nhx1 localizes exclusively to late endosomes, where it transports H^+ and K^+ across the membrane to drive protein trafficking out of the

endosome (Bowers et al., 2000; Brett et al., 2005). Herein, we show that Nhx1 mediates LE trafficking by contributing to LE-vacuole fusion, as knocking out NHX1 impairs this fusion event (Figure 8). Three observations suggest that H^+ transport by Nhx1 underlies its role in LE-vacuole fusion: (1) The pH-dependence of LE-vacuole fusion is shifted to the right for organelles isolated from *nhx1Δ* cells. (2) Replacing Cl^- with acetate, a weak acid, blocks LE-vacuole fusion but only in the absence of NHX1. (3) Treating organelles isolated from *nhx1*Δ cells with chloroquine, a weak base that accumulates within vacuole and LE lumens, suppresses the fusion defect. These results are consistent with the observations that knocking out Nhx1 hyperacidifies the vacuole lumen, and that overcoming this defect with addition of weak base, suppresses protein cargo trafficking defects in vivo (Brett et al., 2005b).

We also found that LE-vacuole and HVF have different monovalent cation profiles, suggesting that different ion transporters contribute to each process. For example, unlike homotypic vacuole fusion, LE-vacuole fusion is supported by Rb^+ (Figure 5D). However, Rb^+ does not support LE-vacuole fusion in the absence of NHX1 (Figure 8C), revealing a condition whereby Nhx1 function is necessary for LE-vacuole fusion. This result is consistent with the finding that Nhx1 is the only transporter on the LE known to transport Rb^+ (Brett et al., 2005b), confirming that its ion exchange activity is important for LE-vacuole fusion.

4. Nhx1 regulates LE-vacuole fusion independent of its interaction with gyp6

Although all predictions were in support of a role for Gyp6 GAP activity in controlling LE-vacuole fusion through its interaction with Nhx1, we found that this interaction was not important at all and knocking out NHX1 had no effect on the activation state of Ypt7 (see Figure 10&11).

It is very possible that Nhx1-Gyp6 interaction is important for LE-TGN fusion which is controlled by Ypt6, the preferred substrate for Gyp6. Notably Nhx1 is found to colocalize 100% with Vps10 (CPY receptor shuttling between LE and TGN) and other TGN markers (Kojima et al., 2012). *nhx1Δ* blocks Vps10 trafficking (Bowers et al., 2000), and disrupts delivery of vacuole cargo proteins through the late endosome. With the new in vitro LE-TGN fusion assay in its way, we might be able to understand the importance of Nhx1-Gyp6 interaction, and perhaps discover the proteins involved in the fusion machinery mediating LE-TGN fusion.

5. Model Summarizing how Nhx1 and the fusion machinery regulate LE-vacuole fusion

In its active state, Ypt7-GTP on the membranes of both the late endosome and the vacuole coordinates the first touch during tethering through their interactions with the VpsC complex. This contact between the two membranes is further strengthened as a result of trans-SNARE pairing between the 3 Q SNAREs (Pep12 on the LE, Vti1 on the vacuole, and the soluble SNARE Vam7), and the vacuolar R SNARE Nyv1 to form the 1R:3Q tarns-SNARE complex needed to merge the phospholipid bilayers, and hence fusion (Figure 12). Omitting a role for Nhx1-Gyp6 interaction in this fusion process, I discuss an alternative mechanism that could be controlled by

Nhx1 to regulate this fusion event. Our preliminary data from Y2H studies (not included in this thesis) show a strong interaction between Nhx1 regulatory C-terminus and Las17 (Actin assembly factor). Notably, actin remodeling is known to be sensitive to change in salt homeostasis and pH (Kang et al., 2012; Eitzen et al., 2002; Maciver et al., 1998) a property regulated by the ionic exchange activity of Nhx1, and thus suggesting a role for actin remodelling early during this fusion process. To test this hypothesis I plan to examine the effect of knocking out NHX1 on the activation state of Cdc42 a Rho-like GTPase that regulates actin remodeling. I will also make a Latrunculin B (drug that binds actin and prevents its depolymerisation) concentration curves in wild type and *nhx1Δ* strains, and I predict that *nhx1Δ* would be more resistant to this drug because the high H^+ proton gradient in the inside relative to the outside of the late endosome lumen is already preventing the depolyemrization of actin.

Because adding a weak base (chloriquine) suppress trafficking defects *in vivo* and LE-vacuole fusion *in vitro* in *nhx1Δ*, this strategy could possibly be used for treatment of patients with loss-of-function mutations in NHE6 and NHE9. Such a treatment could rescue endocytosis defects causing impaired degradation of neurotransmitter receptors at the synapsis of neuron cells, underlying ASDS.

Figure 12. Model describing how Nhx1 regulate LE-vacuole fusion

Ion exchange activity of Nhx1 together with fusion machinery proteins interacts with actin remodeling proteins to regulate LE-vacuole fusion.

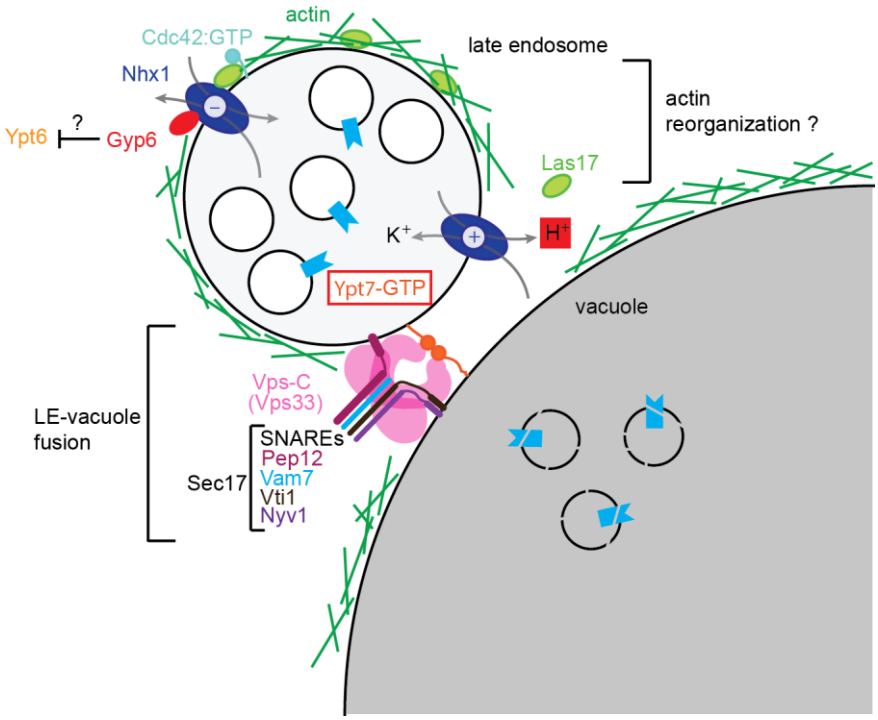
actin
Cdc42:GTP
late endosome
Nhx1
actin
reorganization ?
Ypt6
?
Gyp6
Las17
K+
H+
Ypt7-GTP
vacuole
Vps-C
(Vps33)
LE-vacuole
fusion
SNAREs
Pep12
Sec17
Vam7
Vti1
Nyv1

REFERENCES

Abazeed, M.E., J.M. Blanchette, and R.S. Fuller. 2005. Cell-free transport from the trans-golgi network to late endosome requires factors involved in formation and consumption of clathrin-coated vesicles. *Journal of Biological Chemistry*. 280:4442–50.

Ali, R., C.L. Brett, S. Mukherjee, and R. Rao. 2004. Inhibition of sodium/proton exchange by a Rab-GTPase-activating protein regulates endosomal traffic in yeast. *Journal of Biological Chemistry*. 279:4498–506.

Balderhaar, H.J.K., H. Arlt, C. Ostrowicz, C. Bröcker, F. Sündermann, R. Brandt, M. Babst, and C. Ungermann. 2010. The Rab GTPase Ypt7 is linked to retromer-mediated receptor recycling and fusion at the yeast late endosome. *Journal of Cell Science*. 123:4085–94.

Balderhaar, H.J.K., J. Lachmann, E. Yavavli, C. Bröcker, A. Lürick, and C. Ungermann. 2013. The CORVET complex promotes tethering and fusion of Rab5/Vps21-positive membranes. *Proceedings of the National Academy of Sciences of the United States of America*. 110:3823–8.

Balderhaar, H.J.K., and C. Ungermann. 2013. CORVET and HOPS tethering complexes - coordinators of endosome and lysosome fusion. *Journal of Cell Science*. 126:1307–16.

Barysch, S. V, R. Jahn, and S.O. Rizzoli. 2010. A fluorescence-based in vitro assay for investigating early endosome dynamics. *Nature Protocols*. 5:1127–37.

Bayer, M.J., C. Reese, S. Buhler, C. Peters, and A. Mayer. 2003. Vacuole membrane fusion: V0 functions after trans-SNARE pairing and is coupled to the Ca^{2+}-releasing channel. *Journal of Cell Biology*. 162:211–22.

Becherer, K.A., S.E. Rieder, S.D. Emr, and E.W. Jones. 1996. Novel syntaxin homologue, Pep12p, required for the sorting of lumenal hydrolases to the lysosome-like vacuole in yeast. *Molecular Biology of the Cell*. 7:579–594.

Bensen, E.S., B.G. Yeung, and G.S. Payne. 2001. Ric1p and the Ypt6p GTPase function in a common pathway required for localization of trans-Golgi network membrane proteins. *Molecular Biology of the Cell*. 12:13–26.

Bowers, K., B.P. Levi, F.I. Patel, and T.H. Stevens. 2000. The sodium/proton exchanger Nhx1p is required for endosomal protein trafficking in the yeast Saccharomyces cerevisiae. *Molecular Biology of the Cell*. 11:4277–94.

Brett, C.L., M. Donowitz, R. Rao, and L. Christopher. 2005a. Evolutionary origins of eukaryotic sodium / proton exchangers. *American Journal of Physiology: Cell Physiology* 288:C223-39.

Brett, C.L., and A.J. Merz. 2008. Osmotic regulation of Rab-mediated organelle docking. *Current Biology* 18:1072–7.

Brett, C.L., R.L. Plemel, B.T. Lobingier, B.T. Lobinger, M. Vignali, S. Fields, and A.J. Merz. 2008. Efficient termination of vacuolar Rab GTPase signaling requires coordinated action by a GAP and a protein kinase. *Journal of Cell Biology*. 182:1141–51.

Brett, C.L., D.N. Tukaye, S. Mukherjee, and R. Rao. 2005b. The Yeast Endosomal Na^+(K^+)/H^+ Exchanger Nhx1 Regulates Cellular pH to Control Vesicle Trafficking. *Molecular Biology of the Cell*. 16:1396–1405.

Collins, K.M., and W.T. Wickner. 2007. Trans-SNARE complex assembly and yeast vacuole membrane fusion. *Proceedings of the National Academy of Sciences of the United States of America*. 104:8755–60.

Cunningham, K.W., and G.R. Fink. 1996. Calcineurin inhibits VCX1-dependent H+/Ca2+ exchange and induces Ca2+ ATPases in *Saccharomyces cerevisiae*. *Molecular and Cellular Biology*. 16:2226–37.

Deane, E.C., A.E. Ilie, S. Sizdahkhani, M. Das Gupta, J. Orlowski, and R.A. Mckinney. 2013. Enhanced Recruitment of Endosomal Na^+/ H^+ Exchanger NHE6 into Dendritic Spines of Hippocampal Pyramidal Neurons during NMDA Receptor-Dependent Long-Term Potentiation. *Journal of Neuroscience.* 33:595–610.

Eitzen, G., L. Wang, N. Thorngren, and W. Wickner. 2002. Remodeling of organelle-bound actin is required for yeast vacuole fusion. *Journal of Cell Biology*. 158:669–79.

Franke, B., B.M. Neale, and S. V Faraone. 2009. Genome-wide association studies in ADHD. *Human Genetics*. 126:13–50.

Haas, A., B. Conradt, and W. Wickner. 1994. G-protein ligands inhibit in vitro reactions of vacuole inheritance. *Journal of Cell Biology*. 126:87–97.

Hutagalung, A.H., and P.J. Novick. 2011. Role of Rab GTPases in Membrane Traffic and Cell Physiology. 119–149.

Izawa, R., T. Onoue, N. Furukawa, and J. Mima. 2012. Distinct contributions of vacuolar Qabc- and R-SNARE proteins to membrane fusion specificity. *Journal of Biological Chemistry*. 287:3445–53.

Jun, Y., and W. Wickner. 2007. Assays of vacuole fusion resolve the stages of docking, lipid mixing, and content mixing. *Proceedings of the National Academy of Sciences of the United States of America*. 104:13010–5.

Kang, H., M.J. Bradley, B.R. McCullough, A. Pierre, E.E. Grintsevich, E. Reisler, and E.M. De La Cruz. 2012. Identification of cation-binding sites on actin that drive polymerization and modulate bending stiffness. *Proceedings of the National Academy of Sciences of the United States of America*. 109:16923–7.

Kato, M., and W. Wickner. 2001. Ergosterol is required for the Sec18/ATP-dependent priming step of homotypic vacuole fusion. *EMBO Journal*. 20:4035–40.

Kojima, A., J.Y. Toshima, C. Kanno, C. Kawata, and J. Toshima. 2012. Localization and functional requirement of yeast Na+/H+ exchanger, Nhx1p, in the endocytic and protein recycling pathway. *Biochimica et Biophysica Acta*. 1823:534–43.

Kreis, S., H.-J. Schönfeld, C. Melchior, B. Steiner, and N. Kieffer. 2005. The intermediate filament protein vimentin binds specifically to a recombinant integrin alpha2/beta1 cytoplasmic tail complex and co-localizes with native alpha2/beta1 in endothelial cell focal adhesions. *Experimental Cell Research*. 305:110–21.

Lachmann, J., C. Ungermann, and S. Engelbrecht-Vandré. 2011. Rab GTPases and tethering in the yeast endocytic pathway. *Small GTPases*. 2:182–186.

Lo, S.-Y., C.L. Brett, R.L. Plemel, M. Vignali, S. Fields, T. Gonen, and A.J. Merz. 2011. Intrinsic tethering activity of endosomal Rab proteins. *Nature Structural & Molecular Biology*. 19:40–7.

Longtine, M.S., a McKenzie, D.J. Demarini, N.G. Shah, a Wach, a Brachat, P. Philippsen, and J.R. Pringle. 1998. Additional modules for versatile and economical PCR-based gene deletion and modification in Saccharomyces cerevisiae. *Yeast (Chichester, England)*. 14:953–61.

Maciver, S.K., B.J. Pope, S. Whytock, and a G. Weeds. 1998. The effect of two actin depolymerizing factors (ADF/cofilins) on actin filament turnover: pH sensitivity of F-actin binding by human ADF, but not of Acanthamoeba actophorin. *European Journal of Biochemistry*. 256:388–97.

Mayer, a, W. Wickner, and a Haas. 1996. Sec18p (NSF)-driven release of Sec17p (alpha-SNAP) can precede docking and fusion of yeast vacuoles. *Cell*. 85:83–94.

Merz, A.J., and W.T. Wickner. 2004. Trans-SNARE interactions elicit Ca2+ efflux from the yeast vacuole lumen. *Journal of Cell Biology*. 164:195–206.

Michaillat, L., T.L. Baars, and A. Mayer. 2012. Cell-free reconstitution of vacuole membrane fragmentation reveals regulation of vacuole size and number by TORC1. *Molecular Biology of the Cell*. 23:3438-49.

Morrow, E.M., S. Yoo, S.W. Flavell, T. Kim, Y. Lin, R.S. Hill, N.M. Mukaddes, S. Balkhy, A. Hashmi, S. Al-saad, J. Ware, R.M. Joseph, R. Greenblatt, D. Gleason, J.A. Ertelt, K.A. Apse, J.N. Partlow, B. Barry, H. Yao, K. Markianos, J. Ferland, M.E. Greenberg, and C.A. Walsh. 2008. *Science*. 321:218–223.

Nakamura, N., S. Tanaka, Y. Teko, K. Mitsui, and H. Kanazawa. 2005. Four Na+/H+ exchanger isoforms are distributed to Golgi and post-Golgi compartments and are involved in organelle pH regulation. *Journal of Biological Chemistry*. 280:1561–72.

Nass, R., K.W. Cunningham, and R. Rao 1997. Intracellular Sequestration of Sodium by a Novel Na+/H+ Exchanger in Yeast Is Enhanced by Mutations in the Plasma Membrane H^+-ATPase. *Journal of Biological Chemistry*. 272:26145–26152.

Nass, R., and R. Rao. 1998. Novel Localization of a Na+/H+ Exchanger in a Late Endosomal Compartment of Yeast. *Journal of Biological Chemistry*. 273:21054–21060.

Orlov, S.N., A. V Sitozhevskiĭ, N.I. Pokudin, and V.M. Agnaev. 1985. Mechanism of the effect of EGTA on the affinity to calcium of Ca-transporting and Ca-binding cell systems. *Biokhimiia Moscow Russia*. 50:1920–1925.

Schwartz, M.L., and A.J. Merz. 2009. Capture and release of partially zipped trans-SNARE complexes on intact organelles. *Journal of Cell Biology*. 185:535–49.

Sikorski, R.S., and P. Hieter. 1989. A System of Shuttle Vectors and Yeast Host Strains Designed for Efficient Manipulation of DNA in *Saccharomyces cerevisiae*. *Genetics* 122:19-27

Starai, V.J., Y. Jun, and W. Wickner. 2007. Excess vacuolar SNAREs drive lysis and Rab bypass fusion. *Proceedings of the National Academy of Sciences of the United States of America*.

Starai, V.J., N. Thorngren, R. a Fratti, and W. Wickner. 2005. Ion regulation of homotypic vacuole fusion in Saccharomyces cerevisiae. *Journal of Biological Chemistry*. 280:16754–62.

Stroupe, C., K.M. Collins, R. a Fratti, and W. Wickner. 2006. Purification of active HOPS complex reveals its affinities for phosphoinositides and the SNARE Vam7p. *EMBO Journal*. 25:1579–89.

Summers, S. a, B. a Guebert, and M.F. Shanahan. 1996. Polyphosphoinositide inclusion in artificial lipid bilayer vesicles promotes divalent cation-dependent membrane fusion. *Biophysical Journal*. 71:3199–206.

Szaszi, K., A. Paulsen, E.Z. Szabo, M. Numata, S. Grinstein, and J. Orlowski. 2002. Clathrin-mediated endocytosis and recycling of the neuron-specific Na+/H+ exchanger NHE5 isoform. Regulation by phosphatidylinositol 3'-kinase and the actin cytoskeleton. *Journal of Biological Chemistry*. 277:42623–32.

Thorngren, N., K.M. Collins, R. a Fratti, W. Wickner, and A.J. Merz. 2004. A soluble SNARE drives rapid docking, bypassing ATP and Sec17/18p for vacuole fusion. *EMBO Journal*. 23:2765–76.

Toro, R., M. Konyukh, R. Delorme, C. Leblond, P. Chaste, F. Fauchereau, M. Coleman, M. Leboyer, C. Gillberg, and T. Bourgeron. 2010. Key role for gene dosage and synaptic homeostasis in autism spectrum disorders. *Trends in Genetics* 26:363–72.

Ungermann, C., G.F. Von Mollard, O.N. Jensen, N. Margolis, T.H. Stevens, and W. Wickner. 1999. Three v-SNAREs and two t-SNAREs, present in a pentameric cis-SNARE complex on isolated vacuoles, are essential for homotypic fusion. *Journal of Cell Biology*. 145:1435–1442.

Ungermann, C., and W. Wickner. 1998. Vam7p, a vacuolar SNAP-25 homolog, is required for SNARE complex integrity and vacuole docking and fusion. *EMBO Journal.* 17:3269–3276.

Vollmer, P., E. Will, D. Scheglmann, M. Strom, and D. Gallwitz. 1999. Primary structure and biochemical characterization of yeast GTPase-activating proteins with substrate preference for the transport GTPase Ypt7p. *European journal of Biochemistry*. 260:284–90.

Wang, C.W., P.E. Stromhaug, E.J. Kauffman, L.S. Weisman, and D.J. Klionsky. 2002a. Yeast homotypic vacuole fusion requires the Ccz1-Mon1 complex during the tethering/docking stage. *Journal of Cell Biology*. 163:973–985.

Wang, L., A.J. Merz, K.M. Collins, and W. Wickner. 2002b. Hierarchy of protein assembly at the vertex ring domain for yeast vacuole docking and fusion. *Cell*. 365–374.

Wattiaux, R., N. Laurent, S. Wattiaux-De Coninck, and M. Jadot. 2000. Endosomes, lysosomes: their implication in gene transfer. *Advanced Drug Delivery Reviews*. 41:201–208.

Wickner, W. 2010. Membrane fusion: five lipids, four SNAREs, three chaperones, two nucleotides, and a Rab, all dancing in a ring on yeast vacuoles. *Annual Review of Cell and Developmental Biology*. 26:115–36.

Will, E., and D. Gallwitz. 2001. Biochemical characterization of Gyp6p, a Ypt/Rab-specific GTPase-activating protein from yeast. *Journal of Biological Chemistry*. 276:12135–9.

Xinhan, L., M. Matsushita, M. Numaza, A. Taguchi, K. Mitsui, and H. Kanazawa. 2011. Na^+ / H^+ exchanger isoform 6 (NHE6 / SLC9A6) is involved in clathrin-dependent endocytosis of transferrin. *American Journal of Physiology: Cell Physiology*. 6:1431–1444.